HAL open science

On the Capacity of MIMO Optical Wireless Channels

Longguang Li, Stefan M Moser, Ligong Wang, Michèle Wigger

▶ To cite this version:

Longguang Li, Stefan M Moser, Ligong Wang, Michèle Wigger. On the Capacity of MIMO Optical Wireless Channels. IEEE Transactions on Information Theory, inPress, 10.1109/ITW.2018.8613496 . hal-02310510

HAL Id: hal-02310510

https://telecom-paris.hal.science/hal-02310510

Submitted on 10 Oct 2019

HAL is a multi-disciplinary open access archive for the deposit and dissemination of scientific research documents, whether they are published or not. The documents may come from teaching and research institutions in France or abroad, or from public or private research centers.

L'archive ouverte pluridisciplinaire **HAL**, est destinée au dépôt et à la diffusion de documents scientifiques de niveau recherche, publiés ou non, émanant des établissements d'enseignement et de recherche français ou étrangers, des laboratoires publics ou privés.

On the Capacity of MIMO Optical Wireless Channels

Longguang Li, Stefan M. Moser, Ligong Wang, Michèle Wigger*

18 February 2019

Abstract

This paper studies the capacity of a general multiple-input multiple-output (MIMO) free-space optical intensity channel under a per-input-antenna peak-power constraint and a total average-power constraint over all input antennas. The main focus is on the scenario with more transmit than receive antennas. In this scenario, different input vectors can yield identical distributions at the output, when they result in the same image vector under multiplication by the channel matrix. We first determine the most energy-efficient input vectors that attain each of these image vectors. Based on this, we derive an equivalent capacity expression in terms of the image vector, and establish new lower and upper bounds on the capacity of this channel. The bounds match when the signal-to-noise ratio (SNR) tends to infinity, establishing the high-SNR asymptotic capacity. We also characterize the low-SNR slope of the capacity of this channel.

Index terms — Average- and peak-power constraint, channel capacity, direct detection, Gaussian noise, infrared communication, multiple-input multiple-output (MIMO) channel, optical communication.

1 Introduction

This paper considers an optical wireless communication system where the transmitter modulates the intensity of optical signals coming from light emitting diodes (LEDs) or laser diodes (LDs), and the receiver measures incoming optical intensities by means of photodetectors. Such *intensity-modulation-direct-detection (IM-DD)* systems are appealing because of their simplicity and their good performance at relatively low costs. As a first approximation, the noise in such systems can be assumed to be Gaussian and independent of the transmitted signal. Inputs are nonnegative and typically subject to both peak- and average-power constraints, where the peak-power constraint is mainly due to technical limitations of the used components and where the average-power constraint is imposed by battery limitations and safety considerations. We should notice that, unlike in radio-frequency communication, the average-power constraint applies directly to the transmit signal and not to its square, because the power of the transmit signal is proportional to the optical intensity and hence relates directly to the transmit signal.

IM-DD systems have been extensively studied in recent years [1]–[15], with an increasing interest in multiple-input multiple-output (MIMO) systems where transmitters are equipped with $n_{\mathrm{T}} > 1$ LEDs or LDs and receivers with $n_{\mathrm{R}} > 1$ photo detectors. Practical transmission schemes for such systems with different modulation methods, such as

*L. Li and M. Wigger are with LTCI, Telecom ParisTech, Université Paris-Saclay, 75013 Paris, France. S. Moser is with the Signal and Information Processing Lab, ETH Zurich, Switzerland and with the Institute of Communications Engineering at National Chiao Tung University, Hsinchu, Taiwan. L. Wang is with ETIS—Université Paris Seine, Université de Cergy-Pontoise, ENSEA, CNRS, Cergy-Pontoise, France. This work was presented in parts at the IEEE Information Theory Workshop, Guangzhou, China, November 2018.

pulse-position modulation or LED index modulation based on orthogonal frequency-division multiplexing, were presented in [16]–[18]. Code constructions were described in [19]–[21].

The main focus of this manuscript is on the fundamental limits of MIMO IM-DD systems, more precisely on their *capacity*. In previous works, the capacity of MIMO channels was mostly studied in special cases: 1) the channel matrix has full column rank, i.e., there are fewer transmit than receive antennas: $n_\mathrm{T} \leq n_\mathrm{R}$, and the channel matrix is of rank n_T [11]; 2) the multiple-input single-output (MISO) case where the receiver is equipped with only a single antenna: $n_\mathrm{R} = 1$; and 3) the general MIMO case but with only a peak-power constraint [14] or only an average-power constraint [12], [13]. More specifically, [11] determined the asymptotic capacity at high signal-to-noise ratio (SNR) when the channel matrix is of full column-rank. For general MIMO channels with average-power constraints only, the asymptotic high-SNR capacity was determined in [12], [13]. The coding schemes of [12], [13] were extended to channels with both peak- and average-power constraints, but they were only shown to achieve the high-SNR pre-log (degrees of freedom), and not necessarily the exact asymptotic capacity.

The works most related to ours are [9], [10], [15]. For the MISO case, [9], [10] show that the optimal signaling strategy is to rely as much as possible on antennas with larger channel gains. Specifically, if an antenna is used for active signaling in a channel use, then all antennas with larger channel gains should transmit at maximum allowed peak power A, and all antennas with smaller channel gains should be silenced, i.e., send 0. It is shown that this antenna-cooperation strategy is optimal at all SNRs.

In [15], the asymptotic capacity in the low-SNR regime is considered for general MIMO channels under both a peak- and an average-power constraint. It is shown that the asymptotically-optimal input distribution in the low-SNR regime puts the antennas in a certain order, and assigns positive mass points only to input vectors in $\{0, \mathsf{A}\}^{n_\mathrm{T}}$ in such a way that, if a given input antenna is set to full power A, then also all preceding antennas in the specified order are set to A. This strategy is reminiscent of the optimal signaling strategy for MISO channels [9], [10]. However, whereas the optimal order in [15] needs to be determined numerically, in the MISO case the optimal order naturally follows the channel strengths of the input antennas. Furthermore, the order in [9], [10] is optimal at all SNRs, whereas the order in [15] is shown to be optimal only in the asymptotic low-SNR limit.

The current paper focuses on MIMO channels with more transmit than receive antennas:

$$n_\mathrm{T} > n_\mathrm{R} > 1. \tag{1}$$

Its main contributions are as follows:

1. *Minimum-Energy Signaling:* The optimal signaling strategy for MISO channels of [9], [10] is generalized to MIMO channels with $n_\mathrm{T} > n_\mathrm{R} > 1$. For each "image vector" $\bar{\mathbf{x}}$ — an n_R-dimensional vector that can be produced by multiplying an input vector $\mathbf{x}$ by the channel matrix — Lemma 5 identifies the input vector $\mathbf{x}_{\min}$ that induces $\bar{\mathbf{x}}$ with minimum total energy. The minimum-energy signaling strategy partitions the image space of vectors $\bar{\mathbf{x}}$ into $\binom{n_\mathrm{T}}{n_\mathrm{R}}$ parallelepipeds, each one spanned by a different subset of n_R columns of the channel matrix (see Figures 1 and 2). In each parallelepiped, the minimum-energy signaling sets the $n_\mathrm{T} - n_\mathrm{R}$ inputs corresponding to the columns that were not chosen either to 0 or to A according to a predescribed rule and uses the n_R inputs corresponding to the chosen columns for signaling within the parallelepiped.

2. *Equivalent Capacity Expression:* Using Lemma 5, Proposition 7 expresses the capacity of the MIMO channel in terms of the random image vector $\bar{\mathbf{X}}$. In particular, the power constraints on the input vector are translated into a set of constraints on $\bar{\mathbf{X}}$.

3. *Maximizing the Trace of the Covariance Matrix:* The low-SNR slope of the capacity of the MIMO channel is determined by the trace of the covariance matrix of $\bar{\mathbf{X}}$ [15]. Lemmas 9, 10, and 11 establish several properties for the optimal input distribution that maximizes this trace. They restate the result in [15] that the covariance-trace maximizing input distribution puts positive mass points only on $\{0, \mathsf{A}\}^{n_\mathrm{T}}$ in a way that if an antenna is set to A, then all preceding antennas in a specified order are also set to A. The lemmas restrict the search space for finding the optimal antenna ordering and show that the optimal probability mass function puts nonzero probability to the origin and to at most $n_\mathrm{R} + 1$ other input vectors.

4. *Lower Bounds:* Lower bounds on the capacity of the channel of interest are obtained by applying the Entropy Power Inequality (EPI) [22] and choosing input vectors that maximize the differential entropy of $\bar{\mathbf{X}}$ under the imposed power constraints; see Theorems 14 and 15.

5. *Upper Bounds:* Three capacity upper bounds are derived by means of the equivalent capacity expression in Proposition 7 and the duality-based upper-bounding technique for capacity; see Theorems 16, 17, and 18. Another upper bound uses simple maximum-entropy arguments and algebraic manipulations; see Theorem 19.

6. *Asymptotic Capacity:* Theorem 20 presents the asymptotic capacity when the SNR tends to infinity, and Theorem 21 gives the slope of capacity when the SNR tends to zero. (This later result was already proven in [15], but as described above, our results simplify the computation of the slope.)

The paper is organized as follows. We end the introduction with a few notational conventions. Section 2 provides details of the investigated channel model. Section 3 identifies the minimum-energy signaling schemes. Section 4 provides an equivalent expression for the capacity of the channel. Section 5 shows properties of maximum-variance signaling schemes. Section 6 presents all new lower and upper bounds on the channel capacity, and also gives the high- and low-SNR asymptotics. The paper is concluded in Section 7. Most of the proofs are in the appendices.

Notation: We distinguish between random and deterministic quantities. A random variable is denoted by a capital Roman letter, e.g., Z, while its realization is denoted by the corresponding small Roman letter, e.g., z. Vectors are boldfaced, e.g., $\mathbf{X}$ denotes a random vector and $\mathbf{x}$ its realization. All the matrices in this paper are deterministic, which are denoted in capital letters, and are typeset in a special font, e.g., H. Constants are typeset either in small Romans, in Greek letters, or in a special font, e.g., E or A. Entropy is typeset as $\mathsf{H}(\cdot)$, differential entropy as $\mathsf{h}(\cdot)$, and mutual information as $\mathsf{I}(\cdot;\cdot)$. The relative entropy (Kullback-Leibler divergence) between probability vectors $\mathbf{p}$ and $\mathbf{q}$ is denoted by $\mathsf{D}(\mathbf{p}\|\mathbf{q})$. We will use the $\mathcal{L}_1$-norm, which we indicate by $\|\cdot\|_1$, while $\|\cdot\|_2$ denotes the $\mathcal{L}_2$-norm. The logarithmic function $\log(\cdot)$ denotes the natural logarithm.

2 Channel Model

Consider an $n_\mathrm{R} \times n_\mathrm{T}$ MIMO channel

$$\mathbf{Y} = \mathsf{H}\mathbf{x} + \mathbf{Z}, \tag{2}$$

where $\mathbf{x} = (x_1, \ldots, x_{n_\mathrm{T}})^\mathsf{T}$ denotes the n_T-dimensional channel input vector, where $\mathbf{Z}$ denotes the n_R-dimensional noise vector with independent standard Gaussian entries,

$$\mathbf{Z} \sim \mathcal{N}(0, \mathsf{I}), \tag{3}$$

and where

$$\mathsf{H} = [\mathbf{h}_1, \mathbf{h}_2, \ldots, \mathbf{h}_{n_\mathrm{T}}] \tag{4}$$

is the deterministic $n_\mathrm{R} \times n_\mathrm{T}$ channel matrix with nonnegative entries (hence $\mathbf{h}_1, \ldots, \mathbf{h}_{n_\mathrm{T}}$ are n_R-dimensional column vectors).

The channel inputs correspond to optical intensities sent by the LEDs, hence they are nonnegative:

$$x_k \in \mathbb{R}_0^+, \quad k = 1, \ldots, n_\mathrm{T}. \tag{5}$$

We assume the inputs are subject to a peak-power (peak-intensity) and an average-power (average-intensity) constraint:

$$\Pr\bigl[X_k > \mathsf{A}\bigr] = 0, \quad \forall\, k \in \{1, \ldots, n_\mathrm{T}\}, \tag{6a}$$
$$\mathsf{E}\bigl[\|\mathbf{X}\|_1\bigr] \le \mathsf{E}, \tag{6b}$$

for some fixed parameters $\mathsf{A}, \mathsf{E} > 0$. As mentioned in the introduction, the average-power constraint is on the expectation of the channel input and not on its square. Also note that A describes the maximum power of each single LED, while E describes the allowed total average power of all LEDs together. We denote the ratio between the allowed average power and the allowed peak power by α:

$$\alpha \triangleq \frac{\mathsf{E}}{\mathsf{A}}. \tag{7}$$

Throughout this paper, we assume that

$$\operatorname{rank}(\mathsf{H}) = n_\mathrm{R}. \tag{8}$$

In fact, if $r \triangleq \operatorname{rank}(\mathsf{H})$ is less than n_R, then the receiver can first compute $\mathsf{U}^\mathsf{T}\mathbf{Y}$, where $\mathsf{U}\Sigma\mathsf{V}^\mathsf{T}$ denotes the singular value decomposition of H, and then discard the $n_\mathrm{R} - r$ entries in $\mathsf{U}^\mathsf{T}\mathbf{Y}$ that correspond to zero singular values. The problem is then reduced to one for which (8) holds.[1]

In this paper we are interested in deriving capacity bounds for this channel. The capacity has the standard formula

$$\mathsf{C}_\mathsf{H}(\mathsf{A}, \alpha\mathsf{A}) = \max_{P_\mathbf{X} \text{ satisfying (6)}} \mathrm{I}(\mathbf{X}; \mathbf{Y}). \tag{9}$$

The next proposition shows that, when $\alpha > \frac{n_\mathrm{T}}{2}$, the channel essentially reduces to one with only a peak-power constraint. The other case where $\alpha \le \frac{n_\mathrm{T}}{2}$ will be the main focus of this paper.

Proposition 1. *If $\alpha > \frac{n_\mathrm{T}}{2}$, then the average-power constraint* (6b) *is inactive, i.e.,*

$$\mathsf{C}_\mathsf{H}(\mathsf{A}, \alpha\mathsf{A}) = \mathsf{C}_\mathsf{H}\Bigl(\mathsf{A}, \frac{n_\mathrm{T}}{2}\mathsf{A}\Bigr), \quad \alpha > \frac{n_\mathrm{T}}{2}. \tag{10}$$

If $\alpha \le \frac{n_\mathrm{T}}{2}$, then there exists a capacity-achieving input distribution $P_\mathbf{X}$ in (9) *that satisfies the average-power constraint* (6b) *with equality.*

Proof: See Appendix A. □

We can alternatively write the MIMO channel as

$$\mathbf{Y} = \bar{\mathbf{x}} + \mathbf{Z}, \tag{11}$$

where we set

$$\bar{\mathbf{x}} \triangleq \mathsf{H}\mathbf{x}. \tag{12}$$

[1]A similar approach can be used to handle the case where the components of the noise vector $\mathbf{Z}$ are correlated.

We introduce the following notation. For a matrix $\mathsf{M} = [\mathbf{m}_1, \ldots, \mathbf{m}_k]$, where $\{\mathbf{m}_i\}$ are column vectors, define the set

$$\mathcal{R}(\mathsf{M}) \triangleq \left\{ \sum_{i=1}^{k} \lambda_i \mathbf{m}_i \colon \lambda_1, \ldots, \lambda_k \in [0, \mathsf{A}] \right\}. \tag{13}$$

Note that this set is a *zonotope*. Since the n_{T}-dimensional input vector $\mathbf{x}$ is constrained to the n_{T}-dimensional hypercube $[0, \mathsf{A}]^{n_{\mathrm{T}}}$, the n_{R}-dimensional image vector $\bar{\mathbf{x}}$ takes value in the zonotope $\mathcal{R}(\mathsf{H})$.

For each $\bar{\mathbf{x}} \in \mathcal{R}(\mathsf{H})$, let

$$\mathcal{S}(\bar{\mathbf{x}}) \triangleq \left\{ \mathbf{x} \in [0, \mathsf{A}]^{n_{\mathrm{T}}} : \mathsf{H}\mathbf{x} = \bar{\mathbf{x}} \right\} \tag{14}$$

be the set of input vectors inducing $\bar{\mathbf{x}}$. In the following section we derive the most energy-efficient signaling method to attain a given $\bar{\mathbf{x}}$. This will allow us to express the capacity in terms of $\bar{\mathbf{X}} = \mathsf{H}\mathbf{X}$ instead of $\mathbf{X}$, which will prove useful.

3 Minimum-Energy Signaling

The goal of this section is to identify for every $\bar{\mathbf{x}} \in \mathcal{R}(\mathsf{H})$ the minimum-energy choice of input vector $\mathbf{x}$ that induces $\bar{\mathbf{x}}$. Since the energy of an input vector $\mathbf{x}$ is $\|\mathbf{x}\|_1$, we are interested in finding an $\mathbf{x}_{\min}$ that satisfies

$$\|\mathbf{x}_{\min}\|_1 = \min_{\mathbf{x} \in \mathcal{S}(\bar{\mathbf{x}})} \|\mathbf{x}\|_1. \tag{15}$$

We start by describing (without proof) the choice of $\mathbf{x}_{\min}$ in a 2×3 example.

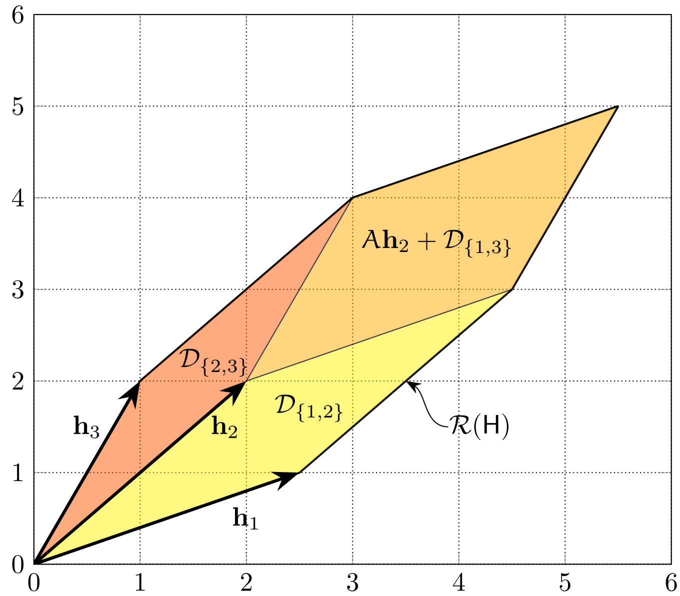

Figure 1: The zonotope $\mathcal{R}(\mathsf{H})$ for the 2×3 MIMO channel matrix $\mathsf{H} = [2.5, 2, 1; 1, 2, 2]$ and its minimum-energy decomposition into three parallelograms.

Example 2. Consider the 2×3 MIMO channel matrix

$$\mathsf{H} = \begin{pmatrix} 2.5 & 2 & 1 \\ 1 & 2 & 2 \end{pmatrix} \tag{16}$$

composed of the three column vectors $\mathbf{h}_1 = (2.5, 1)^\mathsf{T}$, $\mathbf{h}_2 = (2, 2)^\mathsf{T}$, and $\mathbf{h}_3 = (1, 2)^\mathsf{T}$. Figure 1 depicts the zonotope $\mathcal{R}(\mathsf{H})$ and partitions it into three parallelograms based on three different forms of $\mathbf{x}_{\min}$. For any $\bar{\mathbf{x}}$ in the parallelogram $\mathcal{D}_{\{1,2\}} \triangleq \mathcal{R}\big(\mathsf{H}_{\{1,2\}}\big)$, where $\mathsf{H}_{\{1,2\}} \triangleq [\mathbf{h}_1,\ \mathbf{h}_2]$, the minimum-energy input $\mathbf{x}_{\min}$ inducing $\bar{\mathbf{x}}$ has 0 as its third component. Since $\mathsf{H}_{\{1,2\}}$ has full rank, there is only one such input inducing $\bar{\mathbf{x}}$:

$$\mathbf{x}_{\min} = \begin{pmatrix} \mathsf{H}_{\{1,2\}}^{-1}\bar{\mathbf{x}} \\ 0 \end{pmatrix}, \qquad \text{if } \ \bar{\mathbf{x}} \in \mathcal{D}_{\{1,2\}}. \tag{17}$$

Similarly, for any $\bar{\mathbf{x}}$ in the parallelogram $\mathcal{D}_{\{2,3\}} \triangleq \mathcal{R}\big(\mathsf{H}_{\{2,3\}}\big)$, where $\mathsf{H}_{\{2,3\}} \triangleq [\mathbf{h}_2,\ \mathbf{h}_3]$, the minimum-energy input $\mathbf{x}_{\min}$ inducing $\bar{\mathbf{x}}$ has 0 as its first component:

$$\mathbf{x}_{\min} = \begin{pmatrix} 0 \\ \mathsf{H}_{\{2,3\}}^{-1}\bar{\mathbf{x}} \end{pmatrix}, \qquad \text{if } \ \bar{\mathbf{x}} \in \mathcal{D}_{\{2,3\}}. \tag{18}$$

Finally, for any $\bar{\mathbf{x}}$ in the parallelogram $\mathsf{A}\mathbf{h}_2 + \mathcal{D}_{\{1,3\}}$, where $\mathcal{D}_{\{1,3\}} \triangleq \mathcal{R}\big(\mathsf{H}_{\{1,3\}}\big)$ and $\mathsf{H}_{\{1,3\}} \triangleq [\mathbf{h}_1,\ \mathbf{h}_3]$, the minimum-energy input $\mathbf{x}_{\min}$ inducing $\bar{\mathbf{x}}$ has A as its second component:

$$\mathbf{x}_{\min} = \begin{pmatrix} x_{\min,1} \\ \mathsf{A} \\ x_{\min,3} \end{pmatrix}, \qquad \text{if } \ \bar{\mathbf{x}} \in \mathsf{A}\mathbf{h}_2 + \mathcal{D}_{\{1,3\}}, \tag{19}$$

where

$$\begin{pmatrix} x_{\min,1} \\ x_{\min,3} \end{pmatrix} = \mathsf{H}_{\{1,3\}}^{-1}(\bar{\mathbf{x}} - \mathsf{A}\mathbf{h}_2). \tag{20}$$

$\diamondsuit$

We now generalize Example 2 to formally solve the optimization problem in (15) for an arbitrary $n_\mathrm{T} \times n_\mathrm{R}$ channel matrix H. To this end, we need some further definitions. Denote by $\mathcal{U}$ the set of all choices of n_R columns of H that are linearly independent:

$$\mathcal{U} \triangleq \Big\{\mathcal{I} = \{i_1, \ldots, i_{n_\mathrm{R}}\} \subseteq \{1, \ldots, n_\mathrm{T}\} \colon \mathbf{h}_{i_1}, \ldots, \mathbf{h}_{i_{n_\mathrm{R}}} \text{are linearly independent}\Big\}. \tag{21}$$

For every one of these index sets $\mathcal{I} \in \mathcal{U}$, we denote its complement by

$$\mathcal{I}^\mathrm{c} \triangleq \{1, \ldots, n_\mathrm{T}\} \setminus \mathcal{I}; \tag{22}$$

define the $n_\mathrm{R} \times n_\mathrm{R}$ matrix $\mathsf{H}_\mathcal{I}$ containing the columns of H indicated by $\mathcal{I}$:

$$\mathsf{H}_\mathcal{I} \triangleq [\mathbf{h}_i \colon i \in \mathcal{I}]; \tag{23}$$

and define the n_R-dimensional parallelepiped

$$\mathcal{D}_\mathcal{I} \triangleq \mathcal{R}(\mathsf{H}_\mathcal{I}). \tag{24}$$

We shall see (Lemma 5 ahead) that $\mathcal{R}(\mathsf{H})$ can be partitioned into parallelepipeds that are shifted versions of $\{\mathcal{D}_\mathcal{I}\}$ in such a way that, within each parallelepiped, $\mathbf{x}_{\min}$ has the same form, in a sense similar to (17)–(19) in Example 2. To specify our partition, define the n_R-dimensional vector

$$\boldsymbol{\gamma}_{\mathcal{I},j} \triangleq \mathsf{H}_\mathcal{I}^{-1}\mathbf{h}_j, \quad \mathcal{I} \in \mathcal{U},\ j \in \mathcal{I}^\mathrm{c}, \tag{25}$$

and the sum of its components

$$a_{\mathcal{I},j} \triangleq \mathbf{1}_{n_\mathrm{R}}^\mathsf{T}\boldsymbol{\gamma}_{\mathcal{I},j}, \quad \mathcal{I} \in \mathcal{U},\ j \in \mathcal{I}^\mathrm{c}. \tag{26}$$

We next choose a set of coefficients $\{g_{\mathcal{I},j}\}_{\mathcal{I}\in\mathcal{U}, j\in\mathcal{I}^\mathrm{c}}$, which are either 0 or 1, as follows.

- If

$$a_{\mathcal{I},j} \neq 1, \quad \forall \mathcal{I} \in \mathcal{U},\ \forall j \in \mathcal{I}^{\mathrm{c}}, \tag{27}$$

then let

$$g_{\mathcal{I},j} \triangleq \begin{cases} 1 & \text{if } a_{\mathcal{I},j} > 1, \\ 0 & \text{otherwise,} \end{cases} \quad \mathcal{I} \in \mathcal{U},\ j \in \mathcal{I}^{\mathrm{c}}. \tag{28}$$

- If (27) is violated, then run Algorithm 3 below to determine $\{g_{\mathcal{I},j}\}$.

Algorithm 3.

for $j \in \{1, \ldots, n_{\mathrm{T}}\}$ **do**
  for $\mathcal{I} \in \mathcal{U}$ such that $\mathcal{I} \subseteq \{j, \ldots, n_{\mathrm{T}}\}$ **do**
    if $j \in \mathcal{I}^{\mathrm{c}}$ **then**

$$g_{\mathcal{I},j} \triangleq \begin{cases} 1 & \text{if } a_{\mathcal{I},j} \geq 1, \\ 0 & \text{otherwise} \end{cases} \tag{29}$$

    else
      for $k \in \mathcal{I}^{\mathrm{c}} \cap \{j+1, \ldots, n_{\mathrm{T}}\}$ **do**

$$g_{\mathcal{I},k} \triangleq \begin{cases} 1 & \text{if } a_{\mathcal{I},k} > 1 \text{ or } \bigl(a_{\mathcal{I},k} = 1 \text{ and the first component} \\ & \qquad\qquad\qquad \text{of } \boldsymbol{\gamma}_{\mathcal{I},j} \text{ is negative}\bigr), \\ 0 & \text{otherwise} \end{cases} \tag{30}$$

      end for
    end if
  end for
end for

Remark 4. The purpose of Algorithm 3 is to break ties when the minimum in (15) is not unique. Concretely, if (27) is satisfied, then for all $\bar{\mathbf{x}} \in \mathcal{R}(\mathsf{H})$ the input vector that achieves the minimum in (15) is unique. If there exists some $a_{\mathcal{I},j} = 1$, then there may exist multiple equivalent choices. The algorithm simply picks the first one according to a certain order. △

Finally, let

$$\mathbf{v}_{\mathcal{I}} \triangleq \mathsf{A} \sum_{j \in \mathcal{I}^{\mathrm{c}}} g_{\mathcal{I},j} \mathbf{h}_j, \quad \mathcal{I} \in \mathcal{U}. \tag{31}$$

We are now ready to describe our partition of $\mathcal{R}(\mathsf{H})$.

Lemma 5. *Let $\mathcal{D}_{\mathcal{I}}$, $g_{\mathcal{I},j}$, and $\mathbf{v}_{\mathcal{I}}$ be as given in* (24), (28) *or Algorithm 3, and* (31), *respectively.*

1. *The zonotope $\mathcal{R}(\mathsf{H})$ is covered by the parallelepipeds $\{\mathbf{v}_{\mathcal{I}} + \mathcal{D}_{\mathcal{I}}\}_{\mathcal{I} \in \mathcal{U}}$, which overlap only on sets of measure zero:*

$$\bigcup_{\mathcal{I} \in \mathcal{U}} \bigl(\mathbf{v}_{\mathcal{I}} + \mathcal{D}_{\mathcal{I}}\bigr) = \mathcal{R}(\mathsf{H}) \tag{32}$$

and

$$\mathrm{vol}\Bigl(\bigl(\mathbf{v}_{\mathcal{I}} + \mathcal{D}_{\mathcal{I}}\bigr) \cap \bigl(\mathbf{v}_{\mathcal{J}} + \mathcal{D}_{\mathcal{J}}\bigr)\Bigr) = 0, \qquad \mathcal{I} \neq \mathcal{J}, \tag{33}$$

where $\mathrm{vol}(\cdot)$ *denotes the (n_{R}-dimensional) Lebesgue measure.*

2. *Fix some $\mathcal{I} \in \mathcal{U}$ and some $\bar{\mathbf{x}} \in \mathbf{v}_{\mathcal{I}} + \mathcal{D}_{\mathcal{I}}$. The vector that induces $\bar{\mathbf{x}}$ with minimum energy, i.e., $\mathbf{x}_{\min}$ in* (15)*, is given by $\mathbf{x} = (x_1, \dots, x_{n_\mathrm{T}})^\mathsf{T}$, where*

$$x_i = \begin{cases} \mathsf{A} \cdot g_{\mathcal{I},i} & \text{if } i \in \mathcal{I}^\mathrm{c}, \\ \beta_i & \text{if } i \in \mathcal{I}, \end{cases} \tag{34}$$

where the vector $\boldsymbol{\beta} = (\beta_i : i \in \mathcal{I})^\mathsf{T}$ is given by

$$\boldsymbol{\beta} \triangleq \mathsf{H}_{\mathcal{I}}^{-1}(\bar{\mathbf{x}} - \mathbf{v}_{\mathcal{I}}). \tag{35}$$

Proof: See Appendix B. □

Figure 2 shows the partition of $\mathcal{R}(\mathsf{H})$ into the union (32) for two 2×4 examples.

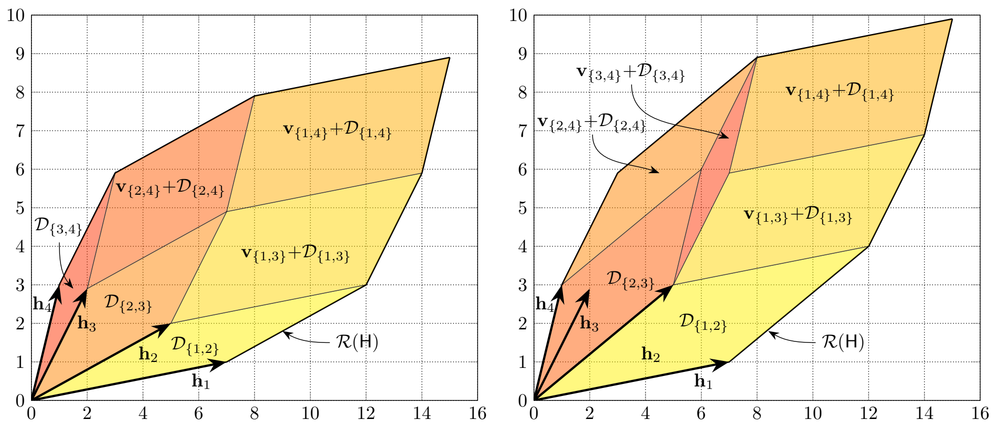

Figure 2: Partition of $\mathcal{R}(\mathsf{H})$ into the union (32) for two 2×4 MIMO examples. The example on the left is for $\mathsf{H} = [7, 5, 2, 1; 1, 2, 2.9, 3]$ and the example on the right for $\mathsf{H} = [7, 5, 2, 1; 1, 3, 2.9, 3]$.

4 Equivalent Capacity Expression

We are now going to state an alternative expression for the capacity $\mathsf{C}_\mathsf{H}(\mathsf{A}, \alpha\mathsf{A})$ in terms of $\bar{\mathbf{X}}$ instead of $\mathbf{X}$. To that goal we define for each index set $\mathcal{I} \in \mathcal{U}$

$$s_{\mathcal{I}} \triangleq \sum_{j \in \mathcal{I}^\mathrm{c}} g_{\mathcal{I},j}, \quad \mathcal{I} \in \mathcal{U}, \tag{36}$$

which indicates the number of components of the input vector set to A in order to induce $\mathbf{v}_{\mathcal{I}}$.

Remark 6. It follows directly from Lemma 5 that

$$0 \leq s_{\mathcal{I}} \leq n_\mathrm{T} - n_\mathrm{R}. \tag{37}$$

△

Proposition 7. *The capacity $\mathsf{C}_\mathsf{H}(\mathsf{A}, \alpha\mathsf{A})$ defined in* (9) *is given by*

$$\mathsf{C}_\mathsf{H}(\mathsf{A}, \alpha\mathsf{A}) = \max_{P_{\bar{\mathbf{X}}}} \mathrm{I}(\bar{\mathbf{X}}; \mathbf{Y}) \tag{38}$$

where the maximization is over all distributions $P_{\bar{\mathbf{X}}}$ over $\mathcal{R}(\mathsf{H})$ subject to the power constraint:

$$\mathsf{E}_U\Big[\mathsf{A} s_U + \big\|\mathsf{H}_U^{-1}\big(\mathsf{E}[\bar{\mathbf{X}} \,|\, U] - \mathbf{v}_U\big)\big\|_1\Big] \leq \alpha\mathsf{A}, \tag{39}$$

where U is a random variable over $\mathcal{U}$ such that[2]

$$\big(U = \mathcal{I}\big) \implies \big(\bar{\mathbf{X}} \in (\mathbf{v}_{\mathcal{I}} + \mathcal{D}_{\mathcal{I}})\big). \tag{40}$$

Proof: Notice that $\bar{\mathbf{X}}$ is a function of $\mathbf{X}$ and that we have a Markov chain $\mathbf{X} \multimap\!\!- \bar{\mathbf{X}} \multimap\!\!- \mathbf{Y}$. Therefore, $\mathrm{I}(\bar{\mathbf{X}};\mathbf{Y}) = \mathrm{I}(\mathbf{X};\mathbf{Y})$. Moreover, by Lemma 5, the range of $\bar{\mathbf{X}}$ in $\mathcal{R}(\mathsf{H})$ can be decomposed into the shifted parallelepipeds $\{\mathbf{v}_{\mathcal{I}} + \mathcal{D}_{\mathcal{I}}\}_{\mathcal{I}\in\mathcal{U}}$. Again by Lemma 5, for any image point $\bar{\mathbf{x}}$ in $\mathbf{v}_{\mathcal{I}} + \mathcal{D}_{\mathcal{I}}$, the minimum energy required to induce $\bar{\mathbf{x}}$ is

$$\mathsf{A}s_{\mathcal{I}} + \left\|\mathsf{H}_{\mathcal{I}}^{-1}(\bar{\mathbf{x}} - \mathbf{v}_{\mathcal{I}})\right\|_1. \tag{41}$$

Without loss in optimality, we restrict ourselves to input vectors $\mathbf{x}$ that achieve some $\bar{\mathbf{x}}$ with minimum energy. Then, by the law of total expectation, the average power can be rewritten as

$$\begin{aligned}
\mathsf{E}\big[\|\mathbf{X}\|_1\big] &= \sum_{\mathcal{I}\in\mathcal{U}} p_{\mathcal{I}}\, \mathsf{E}\big[\|\mathbf{X}\|_1 \,\big|\, U = \mathcal{I}\big] &(42)\\
&= \sum_{\mathcal{I}\in\mathcal{U}} p_{\mathcal{I}}\, \mathsf{E}\Big[\mathsf{A}s_{\mathcal{I}} + \left\|\mathsf{H}_{\mathcal{I}}^{-1}(\bar{\mathbf{X}} - \mathbf{v}_{\mathcal{I}})\right\|_1 \,\Big|\, U = \mathcal{I}\Big] &(43)\\
&= \sum_{\mathcal{I}\in\mathcal{U}} p_{\mathcal{I}} \Big(\mathsf{A}s_{\mathcal{I}} + \left\|\mathsf{H}_{\mathcal{I}}^{-1}\big(\mathsf{E}[\bar{\mathbf{X}}\,|\,U = \mathcal{I}] - \mathbf{v}_{\mathcal{I}}\big)\right\|_1\Big) &(44)\\
&= \mathsf{E}_U\Big[\mathsf{A}s_U + \left\|\mathsf{H}_U^{-1}\big(\mathsf{E}[\bar{\mathbf{X}}\,|\,U] - \mathbf{v}_U\big)\right\|_1\Big]. &(45)
\end{aligned}$$

□

Remark 8. The term inside the expectation on the left-hand side (LHS) of (39) can be seen as a cost function for $\bar{\mathbf{X}}$, where the cost is linear within each of the parallelepipeds $\{\mathcal{D}_{\mathcal{I}} + \mathbf{v}_{\mathcal{I}}\}_{\mathcal{I}\in\mathcal{U}}$ (but not linear on the entire $\mathcal{R}(\mathsf{H})$). At very high SNR, the receiver can obtain an almost perfect guess of U. As a result, our channel can be seen as a set of almost parallel channels in the sense of [22, Exercise 7.28]. Each one of the parallel channels is an amplitude-constrained $n_{\mathrm{R}} \times n_{\mathrm{R}}$ MIMO channel, with a linear power constraint. This observation will help us obtain upper and lower bounds on capacity that are tight in the high-SNR limit. Specifically, for an upper bound, we reveal U to the receiver and then apply previous results on full-rank $n_{\mathrm{R}} \times n_{\mathrm{R}}$ MIMO channels [11]. For a lower bound, we choose the inputs in such a way that, on each parallelepiped $\mathcal{D}_{\mathcal{I}} + \mathbf{v}_{\mathcal{I}}$, the vector $\bar{\mathbf{X}}$ has the high-SNR-optimal distribution for the corresponding $n_{\mathrm{R}} \times n_{\mathrm{R}}$ channel. △

5 Maximum-Variance Signaling

The proofs to the lemmas in this section are given in Appendix C.

As we shall see (Theorem 21 ahead and [15], [23]), at low SNR the asymptotic capacity is characterized by the maximum trace of the covariance matrix of $\bar{\mathbf{X}}$, which we denote

$$\mathsf{K}_{\bar{\mathbf{X}}\bar{\mathbf{X}}} \triangleq \mathsf{E}\big[(\bar{\mathbf{X}} - \mathsf{E}[\bar{\mathbf{X}}])(\bar{\mathbf{X}} - \mathsf{E}[\bar{\mathbf{X}}])^{\mathsf{T}}\big]. \tag{46}$$

In this section we discuss properties of an optimal input distribution for $\mathbf{X}$ that maximizes this trace. Thus, we are interested in the following maximization problem:

$$\max_{P_{\mathbf{X}} \text{ satisfying (6)}} \mathrm{tr}\big(\mathsf{K}_{\bar{\mathbf{X}}\bar{\mathbf{X}}}\big) \tag{47}$$

[2]The choice of U that satisfies (39) is not unique, but U under different choices are equal with probability 1.

where the maximization is over all input distributions $P_{\mathbf{X}}$ satisfying the peak- and average-power constraints given in (6).

The following three lemmas show that the optimal input to the optimization problem in (47) has certain structures: Lemma 9 shows that it is discrete with all entries taking values in $\{0, \mathsf{A}\}$; Lemma 10 shows that the possible values of the optimal $\mathbf{X}$ form a "path" in $[0, \mathsf{A}]^{n_{\mathrm{T}}}$ starting from the origin; and Lemma 11 shows that, under mild assumptions, this optimal $\mathbf{X}$ takes at most $n_{\mathrm{R}} + 2$ values.

Lemma 9. *An optimal input to the maximization problem in* (47) *uses for each component of* $\mathbf{X}$ *only the values* 0 *and* A*:*

$$X_i \in \{0, \mathsf{A}\} \quad \text{with probability } 1, \quad i = 1, \ldots, n_{\mathrm{T}}. \tag{48}$$

Lemma 10. *An optimal input to the optimization problem in* (47) *is a PMF* $P^*_{\mathbf{X}}$ *over a set* $\{\mathbf{x}^*_1, \mathbf{x}^*_2, \ldots\}$ *satisfying*

$$x^*_{k,\ell} \le x^*_{k',\ell} \quad \text{for all } k < k',\ \ell = 1, \ldots, n_{\mathrm{T}}. \tag{49}$$

Furthermore, the first point is $\mathbf{x}^*_1 = \mathbf{0}$*, and*

$$P^*_{\mathbf{X}}(\mathbf{0}) > 0. \tag{50}$$

Notice that Lemma 9 and the first part of Lemma 10 have already been proven in [15]. A proof is given in the appendix for completeness.

Lemma 11. *Define* $\mathcal{T}$ *to be the power set of* $\{1, \ldots, n_{\mathrm{T}}\}$ *without the empty set, and define for every* $\mathcal{J} \in \mathcal{T}$ *and every* $i \in \{1, \ldots, n_{\mathrm{R}}\}$

$$r_{\mathcal{J},i} \triangleq \sum_{k=1}^{n_{\mathrm{T}}} h_{i,k}\, \mathbb{1}\{k \in \mathcal{J}\}, \quad \forall\, \mathcal{J} \in \mathcal{T},\ \forall\, i \in \{1, \ldots, n_{\mathrm{R}}\}. \tag{51}$$

(Here $\mathcal{J}$ *describes a certain choice of input antennas that will be set to* A*, while the remaining antennas will be set to* 0*.) Number all possible* $\mathcal{J} \in \mathcal{T}$ *from* $\mathcal{J}_1$ *to* $\mathcal{J}_{2^{n_{\mathrm{T}}}-1}$ *and define the matrix*

$$\mathsf{R} \triangleq \begin{pmatrix} 2r_{\mathcal{J}_1,1} & \cdots & 2r_{\mathcal{J}_1,n_{\mathrm{R}}} & |\mathcal{J}_1| & \|\mathbf{r}_{\mathcal{J}_1}\|_2^2 \\ 2r_{\mathcal{J}_2,1} & \cdots & 2r_{\mathcal{J}_2,n_{\mathrm{R}}} & |\mathcal{J}_2| & \|\mathbf{r}_{\mathcal{J}_2}\|_2^2 \\ \vdots & \ddots & \vdots & \vdots & \vdots \\ 2r_{\mathcal{J}_{2^{n_{\mathrm{T}}}-1},1} & \cdots & 2r_{\mathcal{J}_{2^{n_{\mathrm{T}}}-1},n_{\mathrm{R}}} & |\mathcal{J}_{2^{n_{\mathrm{T}}}-1}| & \|\mathbf{r}_{\mathcal{J}_{2^{n_{\mathrm{T}}}-1}}\|_2^2 \end{pmatrix} \tag{52}$$

where

$$\mathbf{r}_{\mathcal{J}} \triangleq \bigl(r_{\mathcal{J},1}, r_{\mathcal{J},2}, \ldots, r_{\mathcal{J},n_{\mathrm{R}}}\bigr)^{\mathsf{T}}, \quad \forall\, \mathcal{J} \in \mathcal{T}. \tag{53}$$

Assume that every $(n_{\mathrm{R}} + 2) \times (n_{\mathrm{R}} + 2)$ *submatrix* $\mathsf{R}_{n_{\mathrm{R}}+2}$ *of matrix* R *is full-rank*

$$\operatorname{rank}(\mathsf{R}_{n_{\mathrm{R}}+2}) = n_{\mathrm{R}} + 2, \quad \forall\, \mathsf{R}_{n_{\mathrm{R}}+2}. \tag{54}$$

Then the optimal input to the optimization problem in (47) *is a PMF* $P^*_{\mathbf{X}}$ *over a set* $\{\mathbf{0}, \mathbf{x}^*_1, \ldots, \mathbf{x}^*_{n_{\mathrm{R}}+1}\}$ *with* $n_{\mathrm{R}} + 2$ *points.*

Remark 12. Lemmas 5 and 9 together imply that the optimal $\bar{\mathbf{X}}$ in (47) takes value only in the set $\mathcal{F}_{\mathrm{CP}}$ of corner points of the parallelepipeds $\{\mathbf{v}_{\mathcal{I}} + \mathcal{D}_{\mathcal{I}}\}$:

$$\mathcal{F}_{\mathrm{CP}} \triangleq \bigcup_{\mathcal{I} \in \mathcal{U}} \Bigl\{ \mathbf{v}_{\mathcal{I}} + \sum_{i \in \mathcal{I}} \lambda_i \mathbf{h}_i \colon \lambda_i \in \{0, \mathsf{A}\},\ \forall\, i \in \mathcal{I} \Bigr\}. \tag{55}$$

Lemmas 10 and 11 further imply that the possible values of this optimal $\bar{\mathbf{X}}$ form a path in $\mathcal{F}_{\mathrm{CP}}$, starting from $\mathbf{0}$, and containing no more than $n_{\mathrm{R}} + 2$ points. △

Table 1 (see next page) illustrates four examples of distributions that maximize the trace of the covariance matrix in some MIMO channels.

Table 1: Maximum variance for different channel coefficients

channel gains	α	$\max_{P_{\mathbf{X}}} \operatorname{tr}\big(\mathsf{K}_{\bar{\mathbf{X}}\bar{\mathbf{X}}}\big)$	$P_{\mathbf{X}}\colon \max_{P_{\mathbf{X}}} \operatorname{tr}\big(\mathsf{K}_{\bar{\mathbf{X}}\bar{\mathbf{X}}}\big)$
$\mathsf{H} = \begin{pmatrix} 1.3 & 0.6 & 1 & 0.1 \\ 2.1 & 4.5 & 0.7 & 0.5 \end{pmatrix}$	1.5	$16.3687\mathsf{A}^2$	$P_{\mathbf{X}}(0,0,0,0) = 0.625$, $P_{\mathbf{X}}(\mathsf{A},\mathsf{A},\mathsf{A},\mathsf{A}) = 0.375$
$\mathsf{H} = \begin{pmatrix} 1.3 & 0.6 & 1 & 0.1 \\ 2.1 & 4.5 & 0.7 & 0.5 \end{pmatrix}$	0.9	$12.957\mathsf{A}^2$	$P_{\mathbf{X}}(0,0,0,0) = 0.7$, $P_{\mathbf{X}}(\mathsf{A},\mathsf{A},\mathsf{A},0) = 0.3$
$\mathsf{H} = \begin{pmatrix} 1.3 & 0.6 & 1 & 0.1 \\ 2.1 & 4.5 & 0.7 & 0.5 \end{pmatrix}$	0.6	$9.9575\mathsf{A}^2$	$P_{\mathbf{X}}(0,0,0,0) = 0.7438$, $P_{\mathbf{X}}(\mathsf{A},\mathsf{A},0,0) = 0.1687$, $P_{\mathbf{X}}(\mathsf{A},\mathsf{A},\mathsf{A},0) = 0.0875$
$\mathsf{H} = \begin{pmatrix} 1.3 & 0.6 & 1 & 0.1 \\ 2.1 & 4.5 & 0.7 & 0.5 \end{pmatrix}$	0.3	$6.0142\mathsf{A}^2$	$P_{\mathbf{X}}(0,0,0,0) = 0.85$, $P_{\mathbf{X}}(\mathsf{A},\mathsf{A},0,0) = 0.15$
$\mathsf{H} = \begin{pmatrix} 0.9 & 3.2 & 1 & 2.1 \\ 0.5 & 3.5 & 1.7 & 2.5 \\ 0.7 & 1.1 & 1.1 & 1.3 \end{pmatrix}$	0.9	$23.8405\mathsf{A}^2$	$P_{\mathbf{X}}(0,0,0,0) = 0.7755$, $P_{\mathbf{X}}(\mathsf{A},\mathsf{A},\mathsf{A},\mathsf{A}) = 0.2245$
$\mathsf{H} = \begin{pmatrix} 0.9 & 3.2 & 1 & 2.1 \\ 0.5 & 3.5 & 1.7 & 2.5 \\ 0.7 & 1.1 & 1.1 & 1.3 \end{pmatrix}$	0.75	$20.8950\mathsf{A}^2$	$P_{\mathbf{X}}(0,0,0,0) = 0.7772$, $P_{\mathbf{X}}(\mathsf{A},\mathsf{A},\mathsf{A},0) = 0.1413$, $P_{\mathbf{X}}(\mathsf{A},\mathsf{A},\mathsf{A},\mathsf{A}) = 0.0815$
$\mathsf{H} = \begin{pmatrix} 0.9 & 3.2 & 1 & 2.1 \\ 0.5 & 3.5 & 1.7 & 2.5 \\ 0.7 & 1.1 & 1.1 & 1.3 \end{pmatrix}$	0.6	$17.7968\mathsf{A}^2$	$P_{\mathbf{X}}(0,0,0,0) = 0.8$, $P_{\mathbf{X}}(\mathsf{A},\mathsf{A},\mathsf{A},0) = 0.2$

6 Capacity Results

Define

$$\mathsf{V}_{\mathsf{H}} \triangleq \sum_{\mathcal{I}\in\mathcal{U}} |\det(\mathsf{H}_{\mathcal{I}})|, \tag{56}$$

and let $\mathbf{q}$ be a probability vector on $\mathcal{U}$ with entries

$$q_{\mathcal{I}} \triangleq \frac{|\det \mathsf{H}_{\mathcal{I}}|}{\mathsf{V}_{\mathsf{H}}}, \quad \mathcal{I} \in \mathcal{U}. \tag{57}$$

Further, define

$$\alpha_{\text{th}} \triangleq \frac{n_{\text{R}}}{2} + \sum_{\mathcal{I}\in\mathcal{U}} s_{\mathcal{I}}\, q_{\mathcal{I}}, \tag{58}$$

where $\{s_{\mathcal{I}}\}$ are defined in (36). Notice that α_{th} determines the threshold value for α above which $\bar{\mathbf{X}}$ can be made uniform over $\mathcal{R}(\mathsf{H})$. In fact, combining the minimum-energy signaling in (34) with a uniform distribution for $\bar{\mathbf{X}}$ over $\mathcal{R}(\mathsf{H})$, the expected input power is

$$\begin{aligned}
\mathsf{E}[\|\mathbf{X}\|_1] &= \sum_{\mathcal{I}\in\mathcal{U}} \Pr[U = \mathcal{I}] \cdot \mathsf{E}[\|\mathbf{X}\|_1 \,|\, U = \mathcal{I}] && (59)\\
&= \sum_{\mathcal{I}\in\mathcal{U}} q_{\mathcal{I}} \left(\mathsf{A} s_{\mathcal{I}} + \frac{n_{\text{R}}\mathsf{A}}{2} \right) && (60)\\
&= \alpha_{\text{th}}\mathsf{A} && (61)
\end{aligned}$$

where the random variable U indicates the parallelepiped containing $\bar{\mathbf{X}}$; see (40). Equality (60) holds because, when $\bar{\mathbf{X}}$ is uniform over $\mathcal{R}(\mathsf{H})$, $\Pr[U = \mathcal{I}] = q_{\mathcal{I}}$, and because, conditional on $U = \mathcal{I}$, using the minimum-energy signaling scheme, the input vector $\mathbf{X}$ is uniform over $\mathbf{v}_{\mathcal{I}} + \mathcal{D}_{\mathcal{I}}$.

Remark 13. Note that

$$\alpha_{\text{th}} \leq \frac{n_{\text{T}}}{2}, \tag{62}$$

as can be argued as follows. Let $\mathbf{X}$ be an input that achieves a uniform $\bar{\mathbf{X}}$ with minimum energy. According to (61) it consumes an input power $\alpha_{\text{th}}\mathsf{A}$. Define $\mathbf{X}'$ as

$$X'_i \triangleq \mathsf{A} - X_i, \quad i = 1, \dots, n_{\text{T}}. \tag{63}$$

It must consume input power $(n_{\text{T}} - \alpha_{\text{th}})\mathsf{A}$. Note that $\mathbf{X}'$ also induces a uniform $\bar{\mathbf{X}}$ because the zonotope $\mathcal{R}(\mathsf{H})$ is point-symmetric. Since $\mathbf{X}$ consumes minimum energy, we know

$$\mathsf{E}[\|\mathbf{X}\|_1] \leq \mathsf{E}[\|\mathbf{X}'\|_1], \tag{64}$$

i.e.,

$$\alpha_{\text{th}}\mathsf{A} \leq (n_{\text{T}} - \alpha_{\text{th}})\mathsf{A}, \tag{65}$$

which implies (62). △

6.1 Lower Bounds

The proofs to the theorems in this section can be found in Appendix D.

Theorem 14. *If $\alpha \geq \alpha_{\text{th}}$, then*

$$\mathsf{C}_{\mathsf{H}}(\mathsf{A}, \alpha\mathsf{A}) \geq \frac{1}{2}\log\left(1 + \frac{\mathsf{A}^{2n_{\text{R}}}\mathsf{V}_{\mathsf{H}}^2}{(2\pi e)^{n_{\text{R}}}}\right). \tag{66}$$

Theorem 15. *If $\alpha < \alpha_{\text{th}}$, then*

$$\mathsf{C}_{\mathsf{H}}(\mathsf{A}, \alpha\mathsf{A}) \geq \frac{1}{2}\log\left(1 + \frac{\mathsf{A}^{2n_{\text{R}}}\mathsf{V}_{\mathsf{H}}^2}{(2\pi e)^{n_{\text{R}}}}\, e^{2\nu}\right) \tag{67}$$

with

$$\nu \triangleq \sup_{\lambda \in \left(\max\left\{0, \frac{n_{\text{R}}}{2}+\alpha-\alpha_{\text{th}}\right\}, \min\left\{\frac{n_{\text{R}}}{2}, \alpha\right\}\right)} \left\{ n_{\text{R}}\left(1 - \log\frac{\mu}{1-e^{-\mu}} - \frac{\mu\, e^{-\mu}}{1-e^{-\mu}}\right) - \inf_{\mathbf{p}} \mathsf{D}(\mathbf{p}\|\mathbf{q})\right\}, \tag{68}$$

where μ is the unique solution to the following equation:

$$\frac{1}{\mu} - \frac{e^{-\mu}}{1-e^{-\mu}} = \frac{\lambda}{n_{\text{R}}}, \tag{69}$$

and where the infimum is over all probability vectors $\mathbf{p}$ on $\mathcal{U}$ such that

$$\sum_{\mathcal{I}\in\mathcal{U}} p_{\mathcal{I}} s_{\mathcal{I}} = \alpha - \lambda \tag{70}$$

with $\{s_{\mathcal{I}}\}$ defined in (36).

The two lower bounds in Theorems 14 and 15 are derived by applying the EPI, and by maximizing the differential entropy $\mathsf{h}(\bar{\mathbf{X}})$ under constraints (39). When $\alpha \geq \alpha_{\text{th}}$, choosing $\bar{\mathbf{X}}$ to be uniformly distributed on $\mathcal{R}(\mathsf{H})$ satisfies (39), hence we can achieve $\mathsf{h}(\bar{\mathbf{X}}) = \log \mathsf{V}_{\mathsf{H}}$. When $\alpha < \alpha_{\text{th}}$, the uniform distribution is no longer an admissible distribution for $\bar{\mathbf{X}}$. In this case, we first select a PMF over the events $\{\bar{\mathbf{X}} \in (\mathbf{v}_{\mathcal{I}} + \mathcal{D}_{\mathcal{I}})\}_{\mathcal{I}\in\mathcal{U}}$, and, given $\bar{\mathbf{X}} \in \mathbf{v}_{\mathcal{I}} + \mathcal{D}_{\mathcal{I}}$, we choose the inputs $\{X_i : i \in \mathcal{I}\}$ according to a truncated exponential distribution rotated by the matrix $\mathsf{H}_{\mathcal{I}}$. Interestingly, it is optimal to choose the truncated exponential distributions for all sets $\mathcal{I} \in \mathcal{U}$ to have the same parameter μ. This parameter is determined by the power $\frac{\lambda}{n_{\text{R}}}$ allocated to the n_{R} signaling inputs $\{X_i : i \in \mathcal{I}\}$.

6.2 Upper Bounds

The proofs to the theorems in this section can be found in Appendix E.

The first upper bound is based on an analysis of the channel with peak-power constraint only, i.e., the average-power constraint (6b) is ignored.

Theorem 16. *For an arbitrary α,*

$$\mathsf{C}_{\mathsf{H}}(\mathsf{A}, \alpha\mathsf{A}) \leq \sup_{\mathbf{p}} \left\{ \log \mathsf{V}_{\mathsf{H}} - \mathsf{D}(\mathbf{p}\|\mathbf{q}) + \sum_{\mathcal{I}\in\mathcal{U}} p_{\mathcal{I}} \sum_{\ell=1}^{n_{\text{R}}} \log\left(\sigma_{\mathcal{I},\ell} + \frac{\mathsf{A}}{\sqrt{2\pi e}}\right)\right\}, \tag{71}$$

where $\sigma_{\mathcal{I},\ell}$ denotes the square root of the ℓth diagonal entry of the matrix $\mathsf{H}_{\mathcal{I}}^{-1}\mathsf{H}_{\mathcal{I}}^{-\mathsf{T}}$, and where the supremum is over all probability vectors $\mathbf{p}$ on $\mathcal{U}$.

The following two upper bounds in Theorems 17 and 18 hold only when $\alpha < \alpha_{\text{th}}$.

Theorem 17. *If $\alpha < \alpha_{\text{th}}$, then*

$$\mathsf{C}_{\mathsf{H}}(\mathsf{A}, \alpha\mathsf{A}) \leq \sup_{\mathbf{p}} \inf_{\mu>0} \left\{ \log \mathsf{V}_{\mathsf{H}} - \mathsf{D}(\mathbf{p}\|\mathbf{q}) + \sum_{\mathcal{I}\in\mathcal{U}} p_{\mathcal{I}} \sum_{\ell=1}^{n_{\text{R}}} \log\left(\sigma_{\mathcal{I},\ell} + \frac{\mathsf{A}}{\sqrt{2\pi e}}\frac{1-e^{-\mu}}{\mu}\right)\right.$$

$$+\frac{\mu}{\mathsf{A}\sqrt{2\pi}}\sum_{\mathcal{I}\in\mathcal{U}}p_{\mathcal{I}}\sum_{\ell=1}^{n_{\mathrm{R}}}\sigma_{\mathcal{I},\ell}\left(1-e^{-\frac{\mathsf{A}^2}{2\sigma_{\mathcal{I},\ell}^2}}\right)+\mu\left(\alpha-\sum_{\mathcal{I}\in\mathcal{U}}p_{\mathcal{I}}s_{\mathcal{I}}\right)\Bigg\},\tag{72}$$

where the supremum is over all probability vectors $\mathbf{p}$ *on* $\mathcal{U}$ *such that*

$$\sum_{\mathcal{I}\in\mathcal{U}}p_{\mathcal{I}}s_{\mathcal{I}}\leq\alpha.\tag{73}$$

Theorem 18. *If* $\alpha<\alpha_{\mathrm{th}}$, *then*

$$\begin{aligned}&\mathsf{C_H}(\mathsf{A},\alpha\mathsf{A})\\&\leq\sup_{\mathbf{p}}\inf_{\delta,\mu>0}\Bigg\{\log\mathsf{V_H}-\mathsf{D}(\mathbf{p}\|\mathbf{q})+\sum_{\mathcal{I}\in\mathcal{U}}p_{\mathcal{I}}\sum_{\ell=1}^{n_{\mathrm{R}}}\log\left(\mathsf{A}\cdot\frac{e^{\frac{\mu\delta}{\mathsf{A}}}-e^{-\mu(1+\frac{\delta}{\mathsf{A}})}}{\sqrt{2\pi e}\mu\left(1-2\,\mathcal{Q}\left(\frac{\delta}{\sigma_{\mathcal{I},\ell}}\right)\right)}\right)\\&\quad+\sum_{\mathcal{I}\in\mathcal{U}}p_{\mathcal{I}}\sum_{\ell=1}^{n_{\mathrm{R}}}\mathcal{Q}\left(\frac{\delta}{\sigma_{\mathcal{I},\ell}}\right)+\sum_{\mathcal{I}\in\mathcal{U}}p_{\mathcal{I}}\sum_{\ell=1}^{n_{\mathrm{R}}}\frac{\delta}{\sqrt{2\pi}\sigma_{\mathcal{I},\ell}}e^{-\frac{\delta^2}{2\sigma_{\mathcal{I},\ell}^2}}\\&\quad+\frac{\mu}{\mathsf{A}\sqrt{2\pi}}\sum_{\mathcal{I}\in\mathcal{U}}p_{\mathcal{I}}\sum_{\ell=1}^{n_{\mathrm{R}}}\sigma_{\mathcal{I},\ell}\left(e^{-\frac{\delta^2}{2\sigma_{\mathcal{I},\ell}^2}}-e^{-\frac{(\mathsf{A}+\delta)^2}{2\sigma_{\mathcal{I},\ell}^2}}\right)+\mu\left(\alpha-\sum_{\mathcal{I}\in\mathcal{U}}p_{\mathcal{I}}s_{\mathcal{I}}\right)\Bigg\},\end{aligned}\tag{74}$$

where $\mathcal{Q}(\cdot)$ *denotes the* $\mathcal{Q}$*-function associated with the standard normal distribution, and the supremum is over all probability vectors* $\mathbf{p}$ *on* $\mathcal{U}$ *satisfying* (73).

The three upper bounds in Theorems 16, 17 and 18 are derived using the fact that capacity cannot be larger than over a channel where the receiver observes both $\mathbf{Y}$ and U. The mutual information corresponding to this channel $\mathrm{I}(\bar{\mathbf{X}};\mathbf{Y},U)$ decomposes as $\mathsf{H}(U)+\mathrm{I}(\bar{\mathbf{X}};\mathbf{Y}|U)$, where the term $\mathsf{H}(U)$ indicates the rate that can be achieved by coding over the choice of the parallelepiped to which $\bar{\mathbf{X}}$ belongs, and $\mathrm{I}(\bar{\mathbf{X}};\mathbf{Y}|U)$ indicates the average rate that can be achieved by coding over a single parallelepiped. By the results in Lemma 5, we can treat the channel matrix as an invertible matrix when knowing U, which greatly simplifies the bounding on $\mathrm{I}(\bar{\mathbf{X}};\mathbf{Y}|U)$. The upper bounds are then obtained by optimizing over the probabilities assigned to the different parallelepipeds. As we will see later, the upper bounds are asymptotically tight at high SNR. The reason is that the additional term $\mathrm{I}(\bar{\mathbf{X}};\mathbf{Y},U)-\mathrm{I}(\bar{\mathbf{X}};\mathbf{Y})=\mathrm{I}(\bar{\mathbf{X}};U|\mathbf{Y})$ vanishes as the SNR grows large. To derive the asymptotic high-SNR capacity, we also use previous results in [11], which derived the high-SNR capacity of this channel when the channel matrix is invertible.

Our next upper bound in Theorem 19 is determined by the maximum trace of the covariance matrix of $\bar{\mathbf{X}}$ under constraints (6).

Theorem 19. *For an arbitrary* α,

$$\mathsf{C_H}(\mathsf{A},\alpha\mathsf{A})\leq\frac{n_{\mathrm{R}}}{2}\log\left(1+\frac{1}{n_{\mathrm{R}}}\max_{P_{\mathbf{X}}}\mathrm{tr}\left(\mathsf{K}_{\bar{\mathbf{X}}\bar{\mathbf{X}}}\right)\right),\tag{75}$$

where the maximization is over all input distributions $P_{\mathbf{X}}$ *satisfying the power constraints* (6).

Note that Section 5 provides results that considerably simplify the maximization in (75). In particular, there exists a maximizing $P_{\mathbf{X}}$ that is a probability mass function over $\mathbf{0}$ and at most $n_{\mathrm{R}}+1$ other points on $\mathcal{F}_{\mathrm{CP}}$, where $\mathcal{F}_{\mathrm{CP}}$ is defined in (55).

6.3 Asymptotic Capacity Expressions

The proofs to the theorems in this section can be found in Appendix F.

Theorem 20 (High-SNR Asymptotics). *If $\alpha \geq \alpha_{\text{th}}$, then*

$$\lim_{\mathsf{A}\to\infty} \left\{ \mathsf{C_H}(\mathsf{A}, \alpha\mathsf{A}) - n_{\text{R}} \log \mathsf{A} \right\} = \frac{1}{2} \log\left(\frac{\mathsf{V_H^2}}{(2\pi e)^{n_{\text{R}}}} \right). \tag{76}$$

If $\alpha < \alpha_{\text{th}}$, then

$$\lim_{\mathsf{A}\to\infty} \left\{ \mathsf{C_H}(\mathsf{A}, \alpha\mathsf{A}) - n_{\text{R}} \log \mathsf{A} \right\} = \frac{1}{2} \log\left(\frac{\mathsf{V_H^2}}{(2\pi e)^{n_{\text{R}}}} \right) + \nu, \tag{77}$$

where $\nu < 0$ is defined in (68)–(70).

Recall that α_{th} is a threshold that determines whether $\bar{\mathbf{X}}$ can be uniformly distributed over $\mathcal{R}(\mathsf{H})$ or not. When $\alpha < \alpha_{\text{th}}$, compared with the asymptotic capacity without active average-power constraint, the average-power constraint imposes a penalty on the channel capacity. This penalty is characterized by ν in (77). As shown in Figure 3, ν is a increasing function of α. When $\alpha < \alpha_{\text{th}}$, ν is always negative, and increases to 0 when $\alpha \geq \alpha_{\text{th}}$.

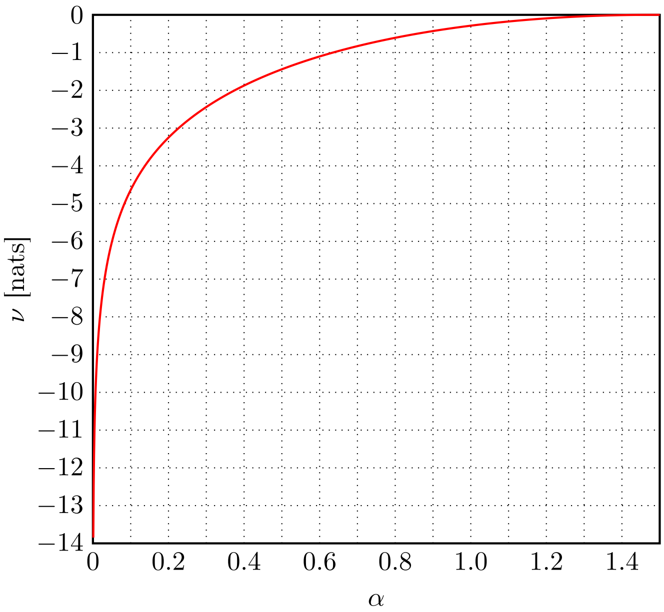

Figure 3: The parameter ν in (68) as a function of α, for a 2×3 MIMO channel with channel matrix $\mathsf{H} = [1, 1.5, 3; 2, 2, 1]$ with corresponding $\alpha_{\text{th}} = 1.4762$. Recall that ν is the asymptotic capacity gap to the case with no active average-power constraint.

Theorem 21 (Low-SNR Asymptotics). *For an arbitrary α,*

$$\lim_{\mathsf{A}\downarrow 0} \frac{\mathsf{C_H}(\mathsf{A}, \alpha\mathsf{A})}{\mathsf{A}^2} = \frac{1}{2} \max_{P_{\mathbf{X}}} \operatorname{tr}\left(\mathsf{K}_{\bar{\mathbf{X}}\bar{\mathbf{X}}}\right), \tag{78}$$

where the maximization is over all input distributions $P_{\mathbf{X}}$ satisfying the power constraints

$$\Pr\left[X_k > 1\right] = 0, \quad \forall\, k \in \{1, \ldots, n_{\text{T}}\}, \tag{79a}$$
$$\mathsf{E}\left[\|\mathbf{X}\|_1\right] \leq \alpha. \tag{79b}$$

Again, see the results in Section 5 about maximizing the trace of the covariance matrix $\mathsf{K}_{\bar{\mathbf{X}}\bar{\mathbf{X}}}$.

Example 22. Figure 4 plots the asymptotic slope, i.e., the right-hand side (RHS) of (78), as a function of α for a 2×3 MIMO channel. As we can see, the asymptotic slope is strictly increasing for all values of $\alpha < \frac{n_{\text{T}}}{2}$. ♢

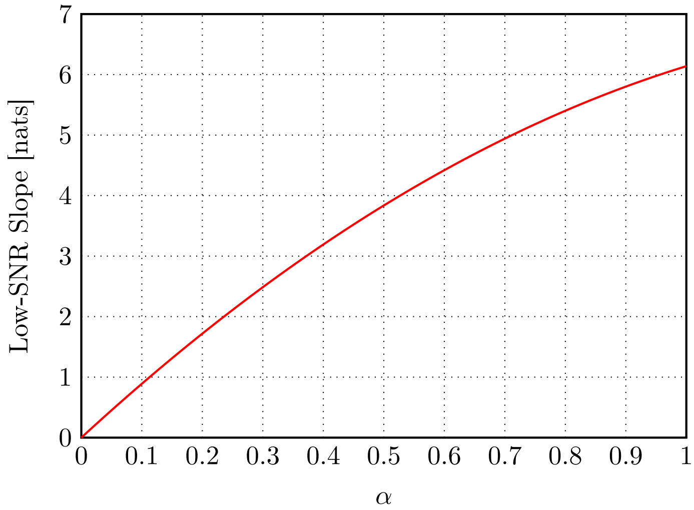

Figure 4: Low-SNR slope as a function of α, for a 2×3 MIMO channel with channel matrix $\mathsf{H} = [1, 1.5, 3; 2, 2, 1]$.

6.4 Numerical Results

In the following we present some numerical examples of our lower and upper bounds.

Example 23. Figures 5 and 6 depict the derived lower and upper bounds for a 2×3 MIMO channel (same channel as in Example 22) for $\alpha = 0.9$ and $\alpha = 0.3$ (both values are less than $\alpha_{\text{th}} = 1.4762$), respectively. Both upper bounds (72) and (74) match with lower bound (67) asymptotically as A tends to infinity. Moreover, upper bound (71) gives a good approximation on capacity when the average-power constraint is weak (i.e., when α is close to α_{th}). Indeed, (71) is asymptotically tight at high SNR when $\alpha \geq \alpha_{\text{th}}$. We also plot three numerical lower bounds by optimizing $\mathrm{I}(\bar{\mathbf{X}}; \mathbf{Y})$ over all feasible choices of $\bar{\mathbf{X}}$ that have positive probability on two, three, or four distinct mass points. (One of the mass points is always at $\mathbf{0}$.) In the low-SNR regime, upper bound (75) matches well with the two-point numerical lower bound. Actually (75) shares the same slope with capacity when the SNR tends to zero, which can be seen by comparing (75) with Theorem 21. $\Diamond$

Example 24. Figures 7 and 8 show similar trends in a 2×4 MIMO channel. Note that although in the 2×3 channel of Figures 5 and 6 the upper bound (72) is always tighter than (74), this does not hold in general, as can be seen in Figure 8. $\Diamond$

7 Concluding Remarks

In this paper, we first express capacity as a maximization problem over distributions for the vector $\bar{\mathbf{X}} = \mathsf{H}\mathbf{X}$. The main challenge there is to transform the total average-power constraint on $\mathbf{X}$ to a constraint on $\bar{\mathbf{X}}$, as the mapping from $\mathbf{x}$ to $\bar{\mathbf{x}}$ is many-to-one. This problem is solved by identifying, for each $\bar{\mathbf{x}}$, the input vector $\mathbf{x}_{\text{min}}$ that induces this $\bar{\mathbf{x}}$ with minimum energy. Specifically, we show that the set $\mathcal{R}(\mathsf{H})$ of all possible $\bar{\mathbf{x}}$ can be decomposed into a number of parallelepipeds such that, for all $\bar{\mathbf{x}}$ within one parallelepiped, the minimum-energy input vectors $\mathbf{x}_{\text{min}}$ have a similar form.

At high SNR, the above minimum-energy signaling result allows the transmitter to decompose the channel into several "almost parallel" channels, each of which being an $n_{\text{R}} \times n_{\text{R}}$ MIMO channel in itself. This is because, at high SNR, the output $\mathbf{y}$ allows the receiver to obtain a good estimate of which of the parallelepipeds $\bar{\mathbf{x}}$ lies in. We can

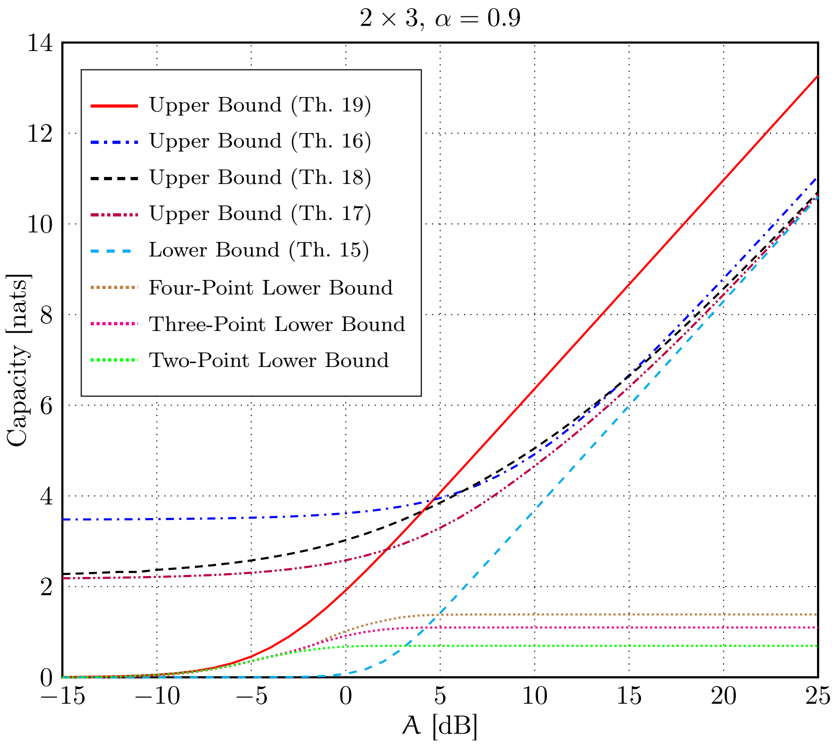

Figure 5: Bounds on capacity of 2×3 MIMO channel with channel matrix $\mathsf{H} = [1, 1.5, 3; 2, 2, 1]$, and average-to-peak power ratio $\alpha = 0.9$. Note that the threshold of the channel is $\alpha_{\text{th}} = 1.4762$.

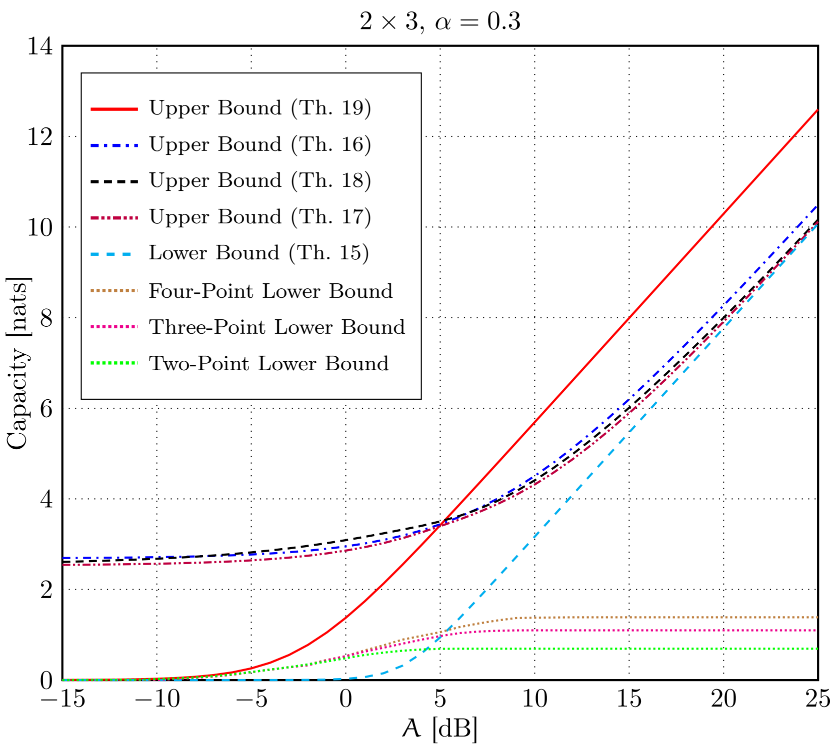

Figure 6: Bounds on capacity of the same 2×3 MIMO channel as discussed in Figure 5, and average-to-peak power ratio $\alpha = 0.3$.

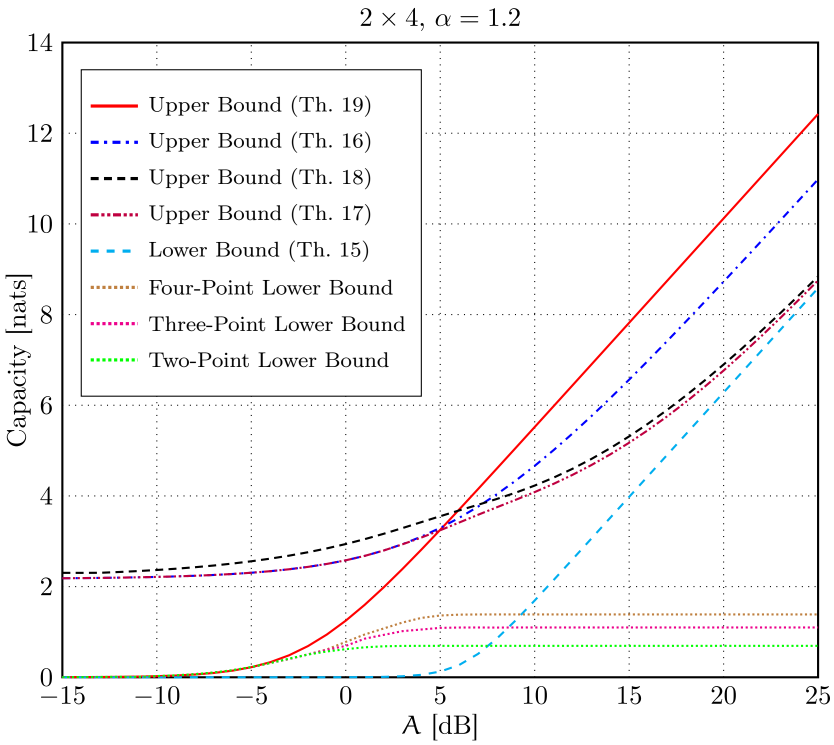

Figure 7: Bounds on capacity of 2×4 MIMO channel with channel matrix $\mathsf{H} = [1.5, 1, 0.75, 0.5; 0.5, 0.75, 1, 1.5]$, and average-to-peak power ratio $\alpha = 1.2$. Note that the threshold of the channel is $\alpha_{\text{th}} = 1.947$.

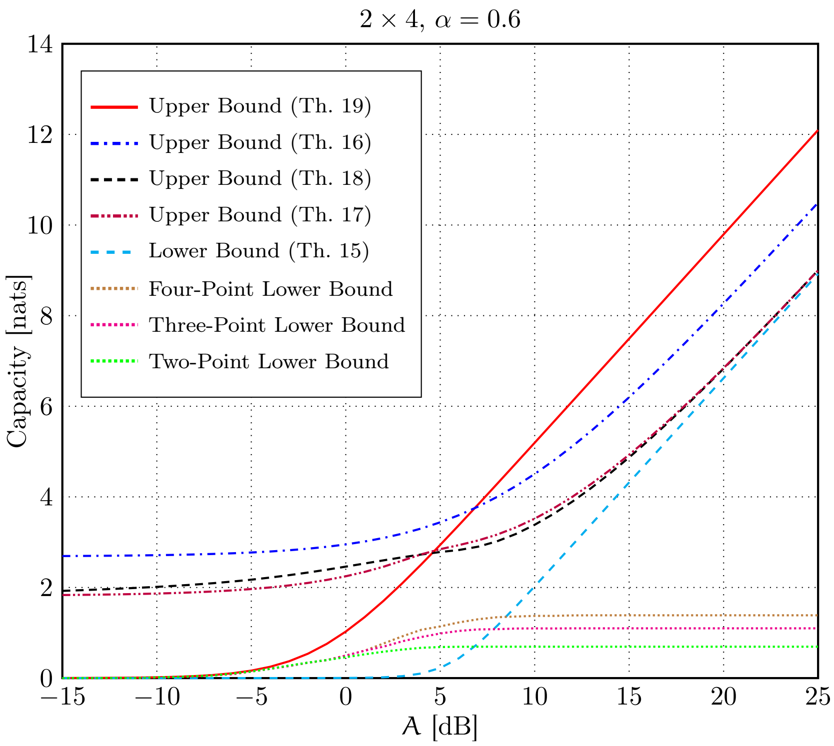

Figure 8: Bounds on capacity of the same 2×4 MIMO channel as discussed in Figure 7, and average-to-peak power ratio $\alpha = 0.6$.

then apply previous results on the capacity of the MIMO channel with full column rank. The remaining steps in deriving our results on the high-SNR asymptotic capacity can be understood, on a high level, as optimizing probabilities and energy constraints assigned to each of the parallel channels.

In the low-SNR regime, the capacity slope is shown to be proportional to the trace of the covariance matrix of $\tilde{\mathbf{X}}$ under the given power constraints. We prove several properties of the input distribution that maximizes this trace. For example, each entry in $\mathbf{X}$ should be either zero or the maximum value A, and the total number of values of $\mathbf{X}$ with nonzero probabilities need not exceed $n_\mathrm{R} + 2$.

Acknowledgment

The authors thank Saïd Ladjal for pointing them to the notion of zonotopes and related literature.

A Proof of Proposition 1

Fix a capacity-achieving input $\mathbf{X}$ and let

$$\alpha^* \triangleq \mathsf{E}\big[\|\mathbf{X}\|_1\big]\mathsf{A}^{-1}. \tag{80}$$

Define $\mathbf{a} \triangleq (\mathsf{A}, \mathsf{A}, \ldots, \mathsf{A})^\mathsf{T}$ and

$$\mathbf{X}' \triangleq \mathbf{a} - \mathbf{X}. \tag{81}$$

We have

$$\mathsf{E}\big[\|\mathbf{X}'\|_1\big] = \mathsf{A}(n_\mathrm{T} - \alpha^*) \tag{82}$$

and

$$\begin{aligned}
\mathrm{I}(\mathbf{X};\mathbf{Y}) &= \mathrm{I}(\mathbf{X};\mathsf{H}\mathbf{a} - \mathbf{Y}) && (83)\\
&= \mathrm{I}(\mathbf{X};\mathsf{H}\mathbf{a} - \mathsf{H}\mathbf{X} - \mathbf{Z}) && (84)\\
&= \mathrm{I}(\mathbf{a} - \mathbf{X};\mathsf{H}(\mathbf{a} - \mathbf{X}) - \mathbf{Z}) && (85)\\
&= \mathrm{I}(\mathbf{a} - \mathbf{X};\mathsf{H}(\mathbf{a} - \mathbf{X}) + \mathbf{Z}) && (86)\\
&= \mathrm{I}(\mathbf{X}';\mathsf{H}\mathbf{X}' + \mathbf{Z}) && (87)\\
&= \mathrm{I}(\mathbf{X}';\mathbf{Y}') && (88)
\end{aligned}$$

where $\mathbf{Y}' \triangleq \mathsf{H}\mathbf{X}' + \mathbf{Z}$, and where (86) follows because $\mathbf{Z}$ is symmetric around $\mathbf{0}$ and independent of $\mathbf{X}$.

Define another random vector $\tilde{\mathbf{X}}$ as follows:

$$\tilde{\mathbf{X}} \triangleq \begin{cases} \mathbf{X} & \text{with probability } p, \\ \mathbf{X}' & \text{with probability } 1-p. \end{cases} \tag{89}$$

Notice that, since $\mathrm{I}(\mathbf{X};\mathbf{Y})$ is concave in $P_\mathbf{X}$ for a fixed channel law, we have

$$\mathrm{I}(\tilde{\mathbf{X}};\tilde{\mathbf{Y}}) \geq p\,\mathrm{I}(\mathbf{X};\mathbf{Y}) + (1-p)\,\mathrm{I}(\mathbf{X}';\mathbf{Y}'). \tag{90}$$

Therefore, by (88),

$$\mathrm{I}(\tilde{\mathbf{X}};\tilde{\mathbf{Y}}) \geq \mathrm{I}(\mathbf{X};\mathbf{Y}) \tag{91}$$

for all $p \in [0, 1]$. Combined with the assumption that $\mathbf{X}$ achieves capacity, (91) implies that $\tilde{\mathbf{X}}$ must also achieve capacity.

We are now ready to prove the two claims in the proposition. We first prove that for $\alpha > \frac{n_{\mathrm{T}}}{2}$ the average-power constraint is inactive. To this end, we choose $p = \frac{1}{2}$, which yields

$$\mathsf{E}\big[\|\tilde{\mathbf{X}}\|_1\big] = \frac{n_{\mathrm{T}}}{2}\mathsf{A}. \tag{92}$$

Since $\tilde{\mathbf{X}}$ achieves capacity (see above), we conclude that capacity is unchanged if one strengthens the average-power constraint from $\alpha\mathsf{A}$ to $\frac{n_{\mathrm{T}}}{2}\mathsf{A}$.

We now prove that, if $\alpha \leq \frac{n_{\mathrm{T}}}{2}$, then there exists a capacity-achieving input distribution for which the average-power constraint is met with equality. Assume that $\alpha^* < \alpha$ (otherwise $\mathbf{X}$ is itself such an input), then choose

$$p = \frac{n_{\mathrm{T}} - \alpha^* - \alpha}{n_{\mathrm{T}} - 2\alpha^*}. \tag{93}$$

With this choice,

$$\begin{aligned} \mathsf{E}\big[\|\tilde{\mathbf{X}}\|_1\big] &= p\,\mathsf{E}\big[\|\mathbf{X}\|_1\big] + (1-p)\,\mathsf{E}\big[\|\mathbf{X}'\|_1\big] && (94)\\ &= \big(p\alpha^* + (1-p)(n_{\mathrm{T}} - \alpha^*)\big)\mathsf{A} && (95)\\ &= \alpha\mathsf{A}. && (96) \end{aligned}$$

Hence $\tilde{\mathbf{X}}$ (which achieves capacity) meets the average-power constraint with equality.

B Proof of Lemma 5

We first restrict ourselves to the case where the condition in (27) is satisfied. The implications caused if (27) is violated are discussed at the end.

We start with Part 2. The minimization problem under consideration,

$$\min_{\mathbf{x}' \in \mathcal{S}(\bar{\mathbf{x}})} \|\mathbf{x}'\|_1, \tag{97}$$

is over a compact set and the objective function is continuous, so a minimum must exist. We are now going to prove that in fact the minimum is unique and is achieved by the input vector $\mathbf{x}$ defined in (34). To that goal, we first link the components β_i in (34) with the components of some arbitrary input vector $\mathbf{x}' \in \mathcal{S}(\bar{\mathbf{x}})$, $\mathbf{x}' \neq \mathbf{x}$, and then use this to show that $\mathbf{x}'$ consumes more energy than $\mathbf{x}$.

In the following, $\mathcal{I}_i$ denotes the ith entry in $\mathcal{I}$ for $i \in \{1, \ldots, n_{\mathrm{R}}\}$. Thus, we can restate (25) as

$$\mathbf{h}_j = \mathsf{H}_{\mathcal{I}}\boldsymbol{\gamma}_{\mathcal{I},j} = \sum_{i=1}^{n_{\mathrm{R}}} \gamma_{\mathcal{I},j}^{(i)}\,\mathbf{h}_{\mathcal{I}_i}, \quad \forall\, j \in \mathcal{I}^{\mathrm{c}}, \tag{98}$$

where $\gamma_{\mathcal{I},j}^{(i)}$, $i = 1, \ldots, n_{\mathrm{R}}$, denote the components of $\boldsymbol{\gamma}_{\mathcal{I},j}$.

So, we choose an arbitrary $\mathbf{x}' \triangleq (x_1', \ldots, x_{n_{\mathrm{T}}}')^{\mathsf{T}} \in \mathcal{S}(\bar{\mathbf{x}})$ and notice that

$$\begin{aligned} \bar{\mathbf{x}} &= \mathsf{H}\mathbf{x}' && (99)\\ &= \sum_{j=1}^{n_{\mathrm{T}}} x_j'\mathbf{h}_j && (100)\\ &= \sum_{j\in\mathcal{I}} x_j'\mathbf{h}_j + \sum_{\substack{j\in\mathcal{I}^{\mathrm{c}}:\\ a_{\mathcal{I},j}<1}} x_j'\mathbf{h}_j + \sum_{\substack{j\in\mathcal{I}^{\mathrm{c}}:\\ a_{\mathcal{I},j}>1}} x_j'\mathbf{h}_j && (101)\\ &= \sum_{j\in\mathcal{I}} x_j'\mathbf{h}_j + \sum_{\substack{j\in\mathcal{I}^{\mathrm{c}}:\\ a_{\mathcal{I},j}<1}} x_j'\mathbf{h}_j + \sum_{\substack{j\in\mathcal{I}^{\mathrm{c}}:\\ a_{\mathcal{I},j}>1}} \mathsf{A}\mathbf{h}_j - \sum_{\substack{j\in\mathcal{I}^{\mathrm{c}}:\\ a_{\mathcal{I},j}>1}} \big(\mathsf{A} - x_j'\big)\mathbf{h}_j && (102) \end{aligned}$$

$$= \sum_{i=1}^{n_\mathrm{R}} x'_{\mathcal{I}_i} \mathbf{h}_{\mathcal{I}_i} + \sum_{\substack{j\in\mathcal{I}^\mathrm{c}:\\ a_{\mathcal{I},j}<1}} x'_j \sum_{i=1}^{n_\mathrm{R}} \gamma_{\mathcal{I},j}^{(i)} \mathbf{h}_{\mathcal{I}_i} + \sum_{\substack{j\in\mathcal{I}^\mathrm{c}:\\ a_{\mathcal{I},j}>1}} \mathsf{A}\mathbf{h}_j - \sum_{\substack{j\in\mathcal{I}^\mathrm{c}:\\ a_{\mathcal{I},j}>1}} \left(\mathsf{A} - x'_j\right) \sum_{i=1}^{n_\mathrm{R}} \gamma_{\mathcal{I},j}^{(i)} \mathbf{h}_{\mathcal{I}_i} \tag{103}$$

$$= \sum_{i=1}^{n_\mathrm{R}} \left(x'_{\mathcal{I}_i} + \sum_{\substack{j\in\mathcal{I}^\mathrm{c}:\\ a_{\mathcal{I},j}<1}} \gamma_{\mathcal{I},j}^{(i)} x'_j - \sum_{\substack{j\in\mathcal{I}^\mathrm{c}:\\ a_{\mathcal{I},j}>1}} \gamma_{\mathcal{I},j}^{(i)} \left(\mathsf{A} - x'_j\right) \right) \mathbf{h}_{\mathcal{I}_i} + \sum_{\substack{j\in\mathcal{I}^\mathrm{c}:\\ a_{\mathcal{I},j}>1}} \mathsf{A}\mathbf{h}_j \tag{104}$$

$$= \sum_{i=1}^{n_\mathrm{R}} \left(x'_{\mathcal{I}_i} + \sum_{\substack{j\in\mathcal{I}^\mathrm{c}:\\ a_{\mathcal{I},j}<1}} \gamma_{\mathcal{I},j}^{(i)} x'_j - \sum_{\substack{j\in\mathcal{I}^\mathrm{c}:\\ a_{\mathcal{I},j}>1}} \gamma_{\mathcal{I},j}^{(i)} \left(\mathsf{A} - x'_j\right) \right) \mathbf{h}_{\mathcal{I}_i} + \mathbf{v}_{\mathcal{I}}, \tag{105}$$

where in (103) we used (98) and where the last equality follows from (28) and (31).

Since $\{\mathbf{h}_i : i \in \mathcal{I}\}$ are linearly independent, they must span $\mathbb{R}^{n_\mathrm{R}}$, and hence the coefficients

$$\left\{ x'_{\mathcal{I}_i} + \sum_{\substack{j\in\mathcal{I}^\mathrm{c}:\\ a_{\mathcal{I},j}<1}} \gamma_{\mathcal{I},j}^{(i)} x'_j - \sum_{\substack{j\in\mathcal{I}^\mathrm{c}:\\ a_{\mathcal{I},j}>1}} \gamma_{\mathcal{I},j}^{(i)} \left(\mathsf{A} - x'_j\right) \right\}_{i\in\{1,\ldots,n_\mathrm{R}\}} \tag{106}$$

uniquely determine $\bar{\mathbf{x}} - \mathbf{v}_{\mathcal{I}}$. Thus it follows from (35) that (106) must be equal to $\{\beta_i\}_{i\in\{1,\ldots,n_\mathrm{R}\}}$, i.e. by (34), to $\{x_{\mathcal{I}_i}\}_{i\in\{1,\ldots,n_\mathrm{R}\}}$.

Next we argue that, if $\mathbf{x}' \neq \mathbf{x}$, then

$$\|\mathbf{x}\|_1 < \|\mathbf{x}'\|_1. \tag{107}$$

To that goal notice that, because the components of $\mathbf{x}$ are nonnegative,

$$\|\mathbf{x}\|_1 = \sum_{j=1}^{n_\mathrm{T}} x_j \tag{108}$$

$$= \sum_{\substack{i\in\mathcal{I}^\mathrm{c}:\\ a_{\mathcal{I},i}>1}} x_i + \sum_{\substack{i\in\mathcal{I}^\mathrm{c}:\\ a_{\mathcal{I},i}<1}} x_i + \sum_{i=1}^{n_\mathrm{R}} x_{\mathcal{I}_i} \tag{109}$$

$$= \sum_{\substack{i\in\mathcal{I}^\mathrm{c}:\\ a_{\mathcal{I},i}>1}} \mathsf{A} + \sum_{\substack{i\in\mathcal{I}^\mathrm{c}:\\ a_{\mathcal{I},i}<1}} 0 + \sum_{i=1}^{n_\mathrm{R}} \left(x'_{\mathcal{I}_i} + \sum_{\substack{j\in\mathcal{I}^\mathrm{c}:\\ a_{\mathcal{I},j}<1}} \gamma_{\mathcal{I},j}^{(i)} x'_j - \sum_{\substack{j\in\mathcal{I}^\mathrm{c}:\\ a_{\mathcal{I},j}>1}} \gamma_{\mathcal{I},j}^{(i)} \left(\mathsf{A} - x'_j\right) \right) \tag{110}$$

$$= \sum_{\substack{j\in\mathcal{I}^\mathrm{c}:\\ a_{\mathcal{I},j}>1}} \mathsf{A} + \sum_{i=1}^{n_\mathrm{R}} x'_{\mathcal{I}_i} + \sum_{\substack{j\in\mathcal{I}^\mathrm{c}:\\ a_{\mathcal{I},j}<1}} \sum_{i=1}^{n_\mathrm{R}} \gamma_{\mathcal{I},j}^{(i)} x'_j - \sum_{\substack{j\in\mathcal{I}^\mathrm{c}:\\ a_{\mathcal{I},j}>1}} \sum_{i=1}^{n_\mathrm{R}} \gamma_{\mathcal{I},j}^{(i)} \left(\mathsf{A} - x'_j\right) \tag{111}$$

$$= \sum_{\substack{j\in\mathcal{I}^\mathrm{c}:\\ a_{\mathcal{I},j}>1}} \mathsf{A} + \sum_{j\in\mathcal{I}} x'_j + \sum_{\substack{j\in\mathcal{I}^\mathrm{c}:\\ a_{\mathcal{I},j}<1}} \underbrace{a_{\mathcal{I},j}}_{<1} x'_j - \sum_{\substack{j\in\mathcal{I}^\mathrm{c}:\\ a_{\mathcal{I},j}>1}} \underbrace{a_{\mathcal{I},j}}_{>1} \left(\mathsf{A} - x'_j\right) \tag{112}$$

$$< \sum_{\substack{j\in\mathcal{I}^\mathrm{c}:\\ a_{\mathcal{I},j}>1}} \mathsf{A} + \sum_{j\in\mathcal{I}} x'_j + \sum_{\substack{j\in\mathcal{I}^\mathrm{c}:\\ a_{\mathcal{I},j}<1}} x'_j - \sum_{\substack{j\in\mathcal{I}^\mathrm{c}:\\ a_{\mathcal{I},j}>1}} (\mathsf{A} - x'_j) \tag{113}$$

$$= \sum_{j=1}^{n_\mathrm{T}} x'_j = \|\mathbf{x}'\|_1. \tag{114}$$

Here (110) follows from (28) and because $\{x_{\mathcal{I}_i}\}$ are identical to (106); (112) follows from (26); and (113) holds because, since $\mathbf{x}' \neq \mathbf{x}$, there must exist some $j \in \mathcal{I}^\mathrm{c}$, $a_{\mathcal{I},j} < 1$, such that $x'_j > 0$, or some $j \in \mathcal{I}^\mathrm{c}$, $a_{\mathcal{I},j} > 1$, such that $x'_j < \mathsf{A}$. This completes the proof of Part 2.

We now prove Part 1. Fix $\mathcal{I}, \mathcal{J} \in \mathcal{U}$ with $\mathcal{I} \neq \mathcal{J}$, and a point $\bar{\mathbf{x}}$ in the interior of $(\mathbf{v}_{\mathcal{I}} + \mathcal{D}_{\mathcal{I}})$. We argue by contradiction that $\bar{\mathbf{x}}$ cannot be in $(\mathbf{v}_{\mathcal{J}} + \mathcal{D}_{\mathcal{J}})$. To this end, choose an index $i \in \{1, \ldots, n_{\mathrm{T}}\}$ such that the channel vector $\mathbf{h}_i$ is in $\mathsf{H}_{\mathcal{I}}$ but not in $\mathsf{H}_{\mathcal{J}}$. Since $\mathcal{I} \neq \mathcal{J}$, such an index must exist. By definition of $\boldsymbol{\beta}$ in (35), any $\mathbf{x}$ that is a solution to the minimization in (97) has x_i lying in the open interval $(0, \mathsf{A})$. If $\bar{\mathbf{x}}$ is also in $(\mathbf{v}_{\mathcal{J}} + \mathcal{D}_{\mathcal{J}})$, then x_i must be 0 or A since $i \in \mathcal{J}^{\mathrm{c}}$. Since we have shown that the solution to the minimization in (97) is unique, we have arrived at a contradiction. Thus, no point can be in the interior of both $(\mathbf{v}_{\mathcal{I}} + \mathcal{D}_{\mathcal{I}})$ and $(\mathbf{v}_{\mathcal{J}} + \mathcal{D}_{\mathcal{J}})$, and therefore their intersection has Lebesgue measure zero.

Furthermore, clearly,

$$\bigcup_{\mathcal{I} \in \mathcal{U}} (\mathbf{v}_{\mathcal{I}} + \mathcal{D}_{\mathcal{I}}) \subseteq \mathcal{R}(\mathsf{H}). \tag{115}$$

Since the intersection of $\mathbf{v}_{\mathcal{I}} + \mathcal{D}_{\mathcal{I}}$ and $\mathbf{v}_{\mathcal{J}} + \mathcal{D}_{\mathcal{J}}$ has Lebesgue measure zero, the reverse direction follows immediately by noting that both sets are closed and

$$\operatorname{vol}\bigl(\mathcal{R}(\mathsf{H})\bigr) = \sum_{\mathcal{I} \in \mathcal{U}} \operatorname{vol}(\mathbf{v}_{\mathcal{I}} + \mathcal{D}_{\mathcal{I}}). \tag{116}$$

This latter equality holds because

$$\operatorname{vol}(\mathbf{v}_{\mathcal{I}} + \mathcal{D}_{\mathcal{I}}) = \mathsf{A}^{n_{\mathrm{R}}} |\det \mathsf{H}_{\mathcal{I}}| \tag{117}$$

and by [24], [25]

$$\operatorname{vol}\bigl(\mathcal{R}(\mathsf{H})\bigr) = \mathsf{A}^{n_{\mathrm{R}}} \sum_{\mathcal{I} \in \mathcal{U}} |\det \mathsf{H}_{\mathcal{I}}|. \tag{118}$$

This completes the proof of Part 1.

Finally, we argue that the lemma holds also when (27) is violated. Note that when $a_{\mathcal{I},j} = 1$ for some $\mathcal{I}$ and j, then the solution to (97) is not necessarily unique anymore. To circumvent this problem, note that Algorithm 3 can be interpreted as generating a small perturbation of the matrix H. We fix some small values $\epsilon_1 > \cdots > \epsilon_{n_{\mathrm{T}}} > 0$ and check through all $a_{\mathcal{I},j}$, $j \in \{1, \ldots, n_{\mathrm{T}}\}$. When we encounter a first tie $a_{\mathcal{I},j} = 1$, we multiply the corresponding vector $\mathbf{h}_j$ by a factor $(1 + \epsilon_1)$ and thereby break the tie (ϵ_1 is chosen to be small enough so that it does not affect any other choices). If a second tie shows up, we use the next perturbation factor $(1 + \epsilon_2)$ (which is smaller than $(1 + \epsilon_1)$, so we do not inadvertently revert our first perturbation); and so on. The lemma is then proven with a continuity argument by letting all of $\epsilon_1, \ldots, \epsilon_{n_{\mathrm{T}}}$ go to zero. We omit the details.

C Proof of Maximum-Variance Signaling Results

C.1 Proof of Lemma 9

The ith diagonal element of $\mathsf{K}_{\bar{\mathbf{X}}\bar{\mathbf{X}}}$ can be decomposed as follows:

$$(\mathsf{K}_{\bar{\mathbf{X}}\bar{\mathbf{X}}})_{i,i} = \mathsf{E}\Bigl[\bigl(\bar{X}_i - \mathsf{E}[\bar{X}_i]\bigr)^2\Bigr] \tag{119}$$

$$= \mathsf{E}\left[\left(\sum_{k=1}^{n_{\mathrm{T}}} h_{i,k}\bigl(X_k - \mathsf{E}[X_k]\bigr)\right)^2\right] \tag{120}$$

$$= \sum_{k=1}^{n_{\mathrm{T}}} h_{i,k}^2 \, \mathsf{E}\Bigl[\bigl(X_k - \mathsf{E}[X_k]\bigr)^2\Bigr] + \sum_{k=1}^{n_{\mathrm{T}}} \sum_{\substack{\ell=1 \\ \ell \neq k}}^{n_{\mathrm{T}}} h_{i,k} h_{i,\ell} \bigl(\mathsf{E}[X_k X_\ell] - \mathsf{E}[X_k]\,\mathsf{E}[X_\ell]\bigr). \tag{121}$$

Thus, the objective function in (47) is

$$\sum_{i=1}^{n_\mathrm{R}} \sum_{k=1}^{n_\mathrm{T}} h_{i,k}^2 \, \mathsf{E}\Big[\big(X_k - \mathsf{E}[X_k]\big)^2\Big] + \sum_{i=1}^{n_\mathrm{R}} \sum_{k=1}^{n_\mathrm{T}} \sum_{\substack{\ell=1\\ \ell\neq k}}^{n_\mathrm{T}} h_{i,k} h_{i,\ell} \big(\mathsf{E}[X_k X_\ell] - \mathsf{E}[X_k]\,\mathsf{E}[X_\ell]\big). \tag{122}$$

If we fix a joint distribution on $(X_1, \ldots, X_{n_\mathrm{T}-1})$ and choose with probability 1 a conditional mean $\mathsf{E}[X_{n_\mathrm{T}} \,|\, X_1, \ldots, X_{n_\mathrm{T}-1}]$, then the consumed total average input power is fixed and every summand on the RHS of (122) is determined except for

$$\mathsf{E}\Big[\big(X_{n_\mathrm{T}} - \mathsf{E}[X_{n_\mathrm{T}}]\big)^2\Big]. \tag{123}$$

This value is maximized—for any choice of joint distribution on $(X_1, \ldots, X_{n_\mathrm{T}-1})$ and conditional mean $\mathsf{E}[X_{n_\mathrm{T}} \,|\, X_1, \ldots, X_{n_\mathrm{T}-1}]$—if X_{n_T} takes value only in the set $\{0, \mathsf{A}\}$. We conclude that, to maximize the expression in (47) subject to a constraint on the average input power, it is optimal to restrict X_{n_T} to taking value only in $\{0, \mathsf{A}\}$.

Repeating this argument for $X_{n_\mathrm{T}-1}$, $X_{n_\mathrm{T}-2}$, etc., we conclude that every X_k, $k = 1, \ldots, n_\mathrm{T}$, should take value only in $\{0, \mathsf{A}\}$.

C.2 Proof of Lemma 10

Some steps in our proof are inspired by [15]. We start by rewriting the objective function in (47) as:

$$\begin{aligned}
\operatorname{tr}\big(\mathsf{K}_{\bar{\mathbf{X}}\bar{\mathbf{X}}}\big) &= \sum_{i=1}^{n_\mathrm{R}} \mathsf{E}\Big[\big(\bar{X}_i - \mathsf{E}[\bar{X}_i]\big)^2\Big] && (124)\\
&= \sum_{i=1}^{n_\mathrm{R}} \mathsf{E}\left[\left(\sum_{k=1}^{n_\mathrm{T}} h_{i,k}\big(X_k - \mathsf{E}[X_k]\big)\right)^2\right] && (125)\\
&= \sum_{i=1}^{n_\mathrm{R}} \sum_{k=1}^{n_\mathrm{T}} \sum_{k'=1}^{n_\mathrm{T}} h_{i,k}\, h_{i,k'}\, \mathsf{E}\big[\big(X_k - \mathsf{E}[X_k]\big)\big(X_{k'} - \mathsf{E}[X_{k'}]\big)\big] && (126)\\
&= \sum_{k=1}^{n_\mathrm{T}} \sum_{k'=1}^{n_\mathrm{T}} \underbrace{\sum_{i=1}^{n_\mathrm{R}} h_{i,k}\, h_{i,k'}}_{\triangleq \kappa_{k,k'}} \cdot \mathsf{Cov}[X_k, X_{k'}] && (127)\\
&= \sum_{k=1}^{n_\mathrm{T}} \sum_{k'=1}^{n_\mathrm{T}} \kappa_{k,k'}\, \mathsf{Cov}[X_k, X_{k'}]. && (128)
\end{aligned}$$

Thus, we need to maximize $\mathsf{Cov}[X_k, X_{k'}]$. Assume that we have fixed the average power E_k, $k = 1, \ldots, n_\mathrm{T}$, assigned to each input antenna, and further assume that we reorder the antennas such that

$$\mathsf{E}_1 \geq \cdots \geq \mathsf{E}_{n_\mathrm{T}}. \tag{129}$$

Note that since each antenna only uses a binary input $X_k \in \{0, \mathsf{A}\}$, the assignment $\mathsf{E}[X_k] = \mathsf{E}_k$ determines the probabilities:

$$\Pr[X_k = \mathsf{A}] = \frac{\mathsf{E}_k}{\mathsf{A}} \tag{130}$$

and the variances:

$$\mathsf{Cov}[X_k, X_k] = \mathsf{Var}[X_k] = \mathsf{E}\big[X_k^2\big] - \mathsf{E}_k^2 = \mathsf{E}_k \mathsf{A} - \mathsf{E}_k^2. \tag{131}$$

For the covariances with $k < k'$ we obtain

$$\mathsf{Cov}[X_k, X_{k'}] = \mathsf{E}[X_k X_{k'}] - \mathsf{E}_k \mathsf{E}_{k'} \tag{132}$$

$$
\begin{aligned}
&= \mathsf{A}^2 \Pr[X_k = X_{k'} = \mathsf{A}] - \mathsf{E}_k \mathsf{E}_{k'} && (133)\\
&= \mathsf{A}^2 \Pr[X_{k'} = \mathsf{A}] \underbrace{\Pr[X_k = \mathsf{A} \,|\, X_{k'} = \mathsf{A}]}_{\leq 1} - \mathsf{E}_k \mathsf{E}_{k'} && (134)\\
&\leq \mathsf{A}\mathsf{E}_{k'} - \mathsf{E}_k \mathsf{E}_{k'} && (135)\\
&= \big(\mathsf{A} - \mathsf{E}_k\big)\mathsf{E}_{k'}. && (136)
\end{aligned}
$$

The upper bound holds with equality if

$$
\Pr[X_k = \mathsf{A} \,|\, X_{k'} = \mathsf{A}] = 1. \tag{137}
$$

This choice is allowed, because for $k < k'$ the ordering (129) is compatible with Condition (137). This proves that the mass points can be ordered in such a way that (49) holds.

We next prove by contradiction that the first mass point must be $\mathbf{0}$. By Lemma 9, if $\mathbf{x}_1^* \neq \mathbf{0}$, then $\mathbf{x}_1^*$ must contain at least one entry that equals A. By (49), that entry must be A for all mass points used by the optimal input. Clearly, changing its value from A to 0 for all mass points will not affect the trace of (46), but will reduce the total input power. Hence we conclude that an input with $\mathbf{x}_1^* \neq \mathbf{0}$ (or with zero probability on $\mathbf{0}$) must be suboptimal.

C.3 Proof of Lemma 11

We investigate the Karush-Kuhn-Tucker (KKT) conditions of the optimization problem (47). Using the definition of $\mathcal{T}$ and $r_{\mathcal{J},i}$ we rewrite the objective function of (47) as

$$
\begin{aligned}
\operatorname{tr}\big(\mathsf{K}_{\bar{\mathbf{X}}\bar{\mathbf{X}}}\big) &= \sum_{i=1}^{n_{\mathrm{R}}} \Big(\mathsf{E}\big[\bar{X}_i^2\big] - \big(\mathsf{E}[\bar{X}_i]\big)^2 \Big) && (138)\\
&= \mathsf{A}^2 \sum_{i=1}^{n_{\mathrm{R}}} \left(\sum_{\mathcal{J}\in\mathcal{T}} p_{\mathcal{J}}\, r_{\mathcal{J},i}^2 - \left(\sum_{\mathcal{J}\in\mathcal{T}} p_{\mathcal{J}}\, r_{\mathcal{J},i} \right)^2 \right). && (139)
\end{aligned}
$$

Taking into account the constraints (6), the Lagrangian is obtained as:

$$
\begin{aligned}
\mathsf{L}(\mathbf{p}, \mu_0, \mu_1, \boldsymbol{\mu}) = \mathsf{A}^2 \sum_{i=1}^{n_{\mathrm{R}}} \left(\sum_{\mathcal{J}\in\mathcal{T}} p_{\mathcal{J}}\, r_{\mathcal{J},i}^2 - \left(\sum_{\mathcal{J}\in\mathcal{T}} p_{\mathcal{J}}\, r_{\mathcal{J},i} \right)^2 \right) - \mu_0 \left(\sum_{\mathcal{J}\in\mathcal{T}} p_{\mathcal{J}} - 1 \right) \\
- \mu_1 \left(\sum_{\mathcal{J}\in\mathcal{T}} p_{\mathcal{J}} |\mathcal{J}| - \alpha \right) - \sum_{\mathcal{J}\in\mathcal{T}} \mu_{\mathcal{J}} (0 - p_{\mathcal{J}}). \qquad (140)
\end{aligned}
$$

The KKT conditions for the optimal PMF $\{p_{\mathcal{K}}^*\}_{\mathcal{K}\in\mathcal{U}}$ are as follows:

$$
\begin{aligned}
\mathsf{A}^2 \sum_{i=1}^{n_{\mathrm{R}}} \left(r_{\mathcal{K},i}^2 - 2 r_{\mathcal{K},i} \sum_{\mathcal{J}\in\mathcal{T}} p_{\mathcal{J}}^*\, r_{\mathcal{J},i} \right) - \mu_0 - \mu_1 |\mathcal{K}| + \mu_{\mathcal{K}} &= 0, \quad \mathcal{K}\in\mathcal{T}, && (141a)\\
\mu_0 \left(\sum_{\mathcal{J}\in\mathcal{T}} p_{\mathcal{J}}^* - 1 \right) &= 0, && (141b)\\
\mu_1 \left(\sum_{\mathcal{J}\in\mathcal{T}} p_{\mathcal{J}}^* |\mathcal{J}| - \alpha \right) &= 0, && (141c)\\
\mu_{\mathcal{K}} p_{\mathcal{K}}^* &= 0, \quad \mathcal{K}\in\mathcal{T}, && (141d)\\
\mu_0 &\geq 0, && (141e)\\
\mu_1 &\geq 0, && (141f)\\
\mu_{\mathcal{K}} &\geq 0, \quad \mathcal{K}\in\mathcal{T}, && (141g)
\end{aligned}
$$

$$\sum_{\mathcal{J}\in\mathcal{T}} p^*_{\mathcal{J}} \leq 1, \tag{141h}$$

$$\sum_{\mathcal{J}\in\mathcal{T}} p^*_{\mathcal{J}} |\mathcal{J}| \leq \alpha, \tag{141i}$$

$$p^*_{\mathcal{K}} \geq 0, \quad \mathcal{K}\in\mathcal{T}. \tag{141j}$$

We define the vector $\mathbf{m} = (m_1, \ldots, m_{n_\mathrm{R}})$ with components

$$m_i \triangleq \sum_{\mathcal{J}\in\mathcal{T}} p^*_{\mathcal{J}} r_{\mathcal{J},i}, \quad i = 1, \ldots, n_\mathrm{R}, \tag{142}$$

and rewrite (141a) as

$$\mathsf{A}^2 \|\mathbf{r}_{\mathcal{K}}\|_2^2 - 2\mathsf{A}^2 \mathbf{r}_{\mathcal{K}}^\mathsf{T}\mathbf{m} - \mu_0 - \mu_1|\mathcal{K}| + \mu_{\mathcal{K}} = 0, \quad \mathcal{K}\in\mathcal{T}. \tag{143}$$

Since by Lemma 10 $P^*_{\mathbf{X}}(\mathbf{0}) > 0$, it must hold that (141h) holds with strict inequality and it thus follows from (141b) that $\mu_0 = 0$.

Next, assume by contradiction that there exist $n_\mathrm{R}+2$ choices $\mathcal{K}_1, \ldots, \mathcal{K}_{n_\mathrm{R}+2} \in \mathcal{T}$ with positive probability $p^*_{\mathcal{K}_\ell} > 0$. Then, by (141d), $\mu_{\mathcal{K}_\ell} = 0$ for all $\ell \in \{1, \ldots, n_\mathrm{R}+2\}$. From (143) we thus have

$$2\mathbf{r}_{\mathcal{K}_\ell}^\mathsf{T}\mathbf{m} + \tilde{\mu}_1|\mathcal{K}_\ell| = \|\mathbf{r}_{\mathcal{K}_\ell}\|_2^2, \quad \ell\in\{1,\ldots,n_\mathrm{R}+2\}, \tag{144}$$

with $\tilde{\mu}_1 \triangleq \mu_1/\mathsf{A}^2$, which can be written in matrix form:

$$\begin{pmatrix} 2r_{\mathcal{K}_1,1} & \cdots & 2r_{\mathcal{K}_1,n_\mathrm{R}} & |\mathcal{K}_1| \\ 2r_{\mathcal{K}_2,1} & \cdots & 2r_{\mathcal{K}_2,n_\mathrm{R}} & |\mathcal{K}_2| \\ \vdots & \ddots & \vdots & \vdots \\ 2r_{\mathcal{K}_{n_\mathrm{R}+2},1} & \cdots & 2r_{\mathcal{K}_{n_\mathrm{R}+2},n_\mathrm{R}} & |\mathcal{K}_{n_\mathrm{R}+2}| \end{pmatrix} \begin{pmatrix} m_1 \\ m_2 \\ \vdots \\ m_{n_\mathrm{R}} \\ \tilde{\mu}_1 \end{pmatrix} = \begin{pmatrix} \|\mathbf{r}_{\mathcal{K}_1}\|_2^2 \\ \|\mathbf{r}_{\mathcal{K}_2}\|_2^2 \\ \vdots \\ \|\mathbf{r}_{\mathcal{K}_{n_\mathrm{R}+2}}\|_2^2 \end{pmatrix}. \tag{145}$$

This is an over-determined system of linear equations in $n_\mathrm{R}+1$ variables $m_1, \ldots, m_{n_\mathrm{R}}, \tilde{\mu}_1$, which has a solution if, and only if,

$$\begin{aligned} &\operatorname{rank}\begin{pmatrix} 2r_{\mathcal{K}_1,1} & \cdots & 2r_{\mathcal{K}_1,n_\mathrm{R}} & |\mathcal{K}_1| \\ 2r_{\mathcal{K}_2,1} & \cdots & 2r_{\mathcal{K}_2,n_\mathrm{R}} & |\mathcal{K}_2| \\ \vdots & \ddots & \vdots & \vdots \\ 2r_{\mathcal{K}_{n_\mathrm{R}+2},1} & \cdots & 2r_{\mathcal{K}_{n_\mathrm{R}+2},n_\mathrm{R}} & |\mathcal{K}_{n_\mathrm{R}+2}| \end{pmatrix} \\ &\quad = \operatorname{rank}\begin{pmatrix} 2r_{\mathcal{K}_1,1} & \cdots & 2r_{\mathcal{K}_1,n_\mathrm{R}} & |\mathcal{K}_1| & \|\mathbf{r}_{\mathcal{K}_1}\|_2^2 \\ 2r_{\mathcal{K}_2,1} & \cdots & 2r_{\mathcal{K}_2,n_\mathrm{R}} & |\mathcal{K}_2| & \|\mathbf{r}_{\mathcal{K}_2}\|_2^2 \\ \vdots & \ddots & \vdots & \vdots & \vdots \\ 2r_{\mathcal{K}_{n_\mathrm{R}+2},1} & \cdots & 2r_{\mathcal{K}_{n_\mathrm{R}+2},n_\mathrm{R}} & |\mathcal{K}_{n_\mathrm{R}+2}| & \|\mathbf{r}_{\mathcal{K}_{n_\mathrm{R}+2}}\|_2^2 \end{pmatrix}. \end{aligned} \tag{146}$$

However, since the matrix on the LHS has only $n_\mathrm{R}+1$ columns, its rank can be at most $n_\mathrm{R}+1$. The matrix on the RHS, on the other hand, has by assumption (see (54)) rank $n_\mathrm{R}+2$. This is a contradiction. We have proven that there exist at most $n_\mathrm{R}+1$ values $p_{\mathcal{K}}$ with positive values. Together with $\mathbf{0}$, there are at most $n_\mathrm{R}+2$ mass points in total.

D Derivation of the Lower Bounds

For any choice of the random vector $\bar{\mathbf{X}}$ over $\mathcal{R}(\mathsf{H})$, the following holds:

$$\begin{aligned} \mathsf{C}_\mathsf{H}(\mathsf{A}, \alpha\mathsf{A}) &\geq \mathrm{I}(\bar{\mathbf{X}}; \bar{\mathbf{X}}+\mathbf{Z}) && (147) \\ &= \mathsf{h}(\bar{\mathbf{X}}+\mathbf{Z}) - \mathsf{h}(\mathbf{Z}) && (148) \end{aligned}$$

$$\geq \frac{1}{2}\log\Big(e^{2\,\mathsf{h}(\bar{\mathbf{X}})} + e^{2\,\mathsf{h}(\mathbf{Z})}\Big) - \mathsf{h}(\mathbf{Z}) \tag{149}$$

$$= \frac{1}{2}\log\left(1 + \frac{e^{2\,\mathsf{h}(\bar{\mathbf{X}})}}{(2\pi e)^{n_{\mathrm{R}}}}\right), \tag{150}$$

where (149) follows from the EPI [22].

D.1 Proof of Theorem 14

We choose $\bar{\mathbf{X}}$ to be uniformly distributed over $\mathcal{R}(\mathsf{H})$. To verify that this uniform distribution satisfies the average-power constraint (39), we define

$$p_{\mathcal{I}} \triangleq \Pr[U = \mathcal{I}] \tag{151}$$

and derive

$$\begin{aligned}
&\mathsf{E}_U\big[\mathsf{A} s_U + \big\|\mathsf{H}_U^{-1}\big(\mathsf{E}\big[\bar{\mathbf{X}}\big|U\big] - \mathbf{v}_U\big)\big\|_1\big] \\
&\quad = \mathsf{A}\sum_{\mathcal{I}\in\mathcal{U}} p_{\mathcal{I}}\, s_{\mathcal{I}} + \sum_{\mathcal{I}\in\mathcal{U}} p_{\mathcal{I}}\big\|\mathsf{H}_{\mathcal{I}}^{-1}\big(\mathsf{E}[\bar{\mathbf{X}}|U=\mathcal{I}] - \mathbf{v}_{\mathcal{I}}\big)\big\|_1 && (152)\\
&\quad = \mathsf{A}\sum_{\mathcal{I}\in\mathcal{U}} q_{\mathcal{I}}\, s_{\mathcal{I}} + \sum_{\mathcal{I}\in\mathcal{U}} q_{\mathcal{I}} \cdot \frac{n_{\mathrm{R}}\mathsf{A}}{2} && (153)\\
&\quad = \alpha_{\mathrm{th}}\mathsf{A} && (154)\\
&\quad \leq \alpha\mathsf{A}. && (155)
\end{aligned}$$

Here, (153) follows because when $\bar{\mathbf{X}}$ is uniformly distributed in $\mathcal{R}(\mathsf{H})$, we have

$$\mathsf{H}_{\mathcal{I}}^{-1}\big(\mathsf{E}[\bar{\mathbf{X}}|U=\mathcal{I}] - \mathbf{v}_{\mathcal{I}}\big) = \frac{\mathsf{A}}{2}\cdot \mathbf{1}_{n_{\mathrm{R}}} \tag{156}$$

and

$$p_{\mathcal{I}} = q_{\mathcal{I}}, \quad \mathcal{I}\in\mathcal{U}. \tag{157}$$

Further, (154) holds because of (58), and the last inequality (155) holds by the assumption in the theorem.

The uniform distribution of $\bar{\mathbf{X}}$ results in

$$\mathsf{h}(\bar{\mathbf{X}}) = \log(\mathsf{A}^{n_{\mathrm{R}}}\cdot \mathsf{V}_{\mathsf{H}}), \tag{158}$$

which, by (150), leads to (66).

D.2 Proof of Theorem 15

We choose

$$\lambda \in \left(\max\left\{0, \frac{n_{\mathrm{R}}}{2} + \alpha - \alpha_{\mathrm{th}}\right\}, \min\left\{\frac{n_{\mathrm{R}}}{2}, \alpha\right\}\right), \tag{159}$$

a probability vector $\mathbf{p}$ satisfying (70), and μ as the unique solution to (69).

Note that such choices are always possible as can be argued as follows. From (159) one directly sees that $0 < \lambda < \frac{n_{\mathrm{R}}}{2}$. Thus, $0 < \frac{\lambda}{n_{\mathrm{R}}} < \frac{1}{2}$, which corresponds exactly to the range where (69) has a unique solution. From (159) it also follows that $\frac{n_{\mathrm{R}}}{2} + \alpha - \alpha_{\mathrm{th}} < \lambda < \alpha$ and thus

$$0 < \alpha - \lambda < \alpha_{\mathrm{th}} - \frac{n_{\mathrm{R}}}{2} \leq \frac{n_{\mathrm{T}}}{2} - \frac{n_{\mathrm{R}}}{2}, \tag{160}$$

where the inequality follows from (62). So the RHS of (70) takes value within the interval $\big(0, \frac{n_{\mathrm{T}}-n_{\mathrm{R}}}{2}\big)$. By Remark 6, the LHS of (70) can take value in the interval $[0, n_{\mathrm{T}} - n_{\mathrm{R}}]$, which covers the range of the RHS. The existence of $\mathbf{p}$ satisfying (70) now follows from the continuity of the LHS of (70) in $\mathbf{p}$.

For each $\mathcal{I}$ we now pick the probability density function (PDF) $f_{\bar{\mathbf{X}}|U=\mathcal{I}}$ to be the n_{R}-dimensional product truncated exponential distribution rotated by the matrix $\mathsf{H}_{\mathcal{I}}$:

$$f_{\bar{\mathbf{X}}|U=\mathcal{I}}(\bar{\mathbf{x}}) = \frac{1}{\mathsf{A}^{n_{\mathrm{R}}}|\det \mathsf{H}_{\mathcal{I}}|} \cdot \left(\frac{\mu}{1-e^{-\mu}}\right)^{n_{\mathrm{R}}} e^{\frac{-\mu\|\mathsf{H}_{\mathcal{I}}^{-1}(\bar{\mathbf{x}}-\mathbf{v}_{\mathcal{I}})\|_1}{\mathsf{A}}}. \tag{161}$$

Note that this corresponds to the entropy-maximizing distribution under a total average-power constraint. The average-power constraint (39) is satisfied because

$$\begin{aligned}
&\mathsf{E}_U\big[\mathsf{A}s_U + \big\|\mathsf{H}_U^{-1}\big(\mathsf{E}\big[\bar{\mathbf{X}}\,\big|\,U\big] - \mathbf{v}_U\big)\big\|_1\big] \\
&\quad = \sum_{\mathcal{I}\in\mathcal{U}} p_{\mathcal{I}}\Big(\mathsf{A}s_{\mathcal{I}} + \big\|\mathsf{H}_{\mathcal{I}}^{-1}\big(\mathsf{E}[\bar{\mathbf{X}}\,|\,U=\mathcal{I}] - \mathbf{v}_{\mathcal{I}}\big)\big\|_1\Big) &(162)\\
&\quad = \sum_{\mathcal{I}\in\mathcal{U}} p_{\mathcal{I}}\bigg(\mathsf{A}s_{\mathcal{I}} + n_{\mathrm{R}}\mathsf{A}\bigg(\frac{1}{\mu} - \frac{e^{-\mu}}{1-e^{-\mu}}\bigg)\bigg) &(163)\\
&\quad = \sum_{\mathcal{I}\in\mathcal{U}} p_{\mathcal{I}}\big(\mathsf{A}s_{\mathcal{I}} + \mathsf{A}\lambda\big) &(164)\\
&\quad = \mathsf{A}\sum_{\mathcal{I}\in\mathcal{U}} p_{\mathcal{I}}s_{\mathcal{I}} + \mathsf{A}\lambda &(165)\\
&\quad = \mathsf{A}(\alpha-\lambda) + \mathsf{A}\lambda &(166)\\
&\quad = \alpha\mathsf{A}. &(167)
\end{aligned}$$

Here, (163) follows from the expected value of the truncated exponential distribution; (164) is due to (69); and (166) follows from (70).

Furthermore,

$$\begin{aligned}
\mathsf{h}(\bar{\mathbf{X}}) &= \mathrm{I}(\bar{\mathbf{X}};U) + \mathsf{h}(\bar{\mathbf{X}}|U) &(168)\\
&= \mathsf{H}(U) + \mathsf{h}(\bar{\mathbf{X}}|U) &(169)\\
&= \mathsf{H}(\mathbf{p}) + \sum_{\mathcal{I}\in\mathcal{U}} p_{\mathcal{I}}\,\mathsf{h}(\bar{\mathbf{X}}|U=\mathcal{I}) &(170)\\
&= \mathsf{H}(\mathbf{p}) + \sum_{\mathcal{I}\in\mathcal{U}} p_{\mathcal{I}}\log|\det\mathsf{H}_{\mathcal{I}}| + n_{\mathrm{R}}\log\mathsf{A} - n_{\mathrm{R}}\log\frac{\mu}{1-e^{-\mu}} \\
&\quad + n_{\mathrm{R}}\bigg(1 - \frac{\mu\, e^{-\mu}}{1-e^{-\mu}}\bigg) &(171)\\
&= -\sum_{\mathcal{I}\in\mathcal{U}} p_{\mathcal{I}}\log p_{\mathcal{I}} + \sum_{\mathcal{I}\in\mathcal{U}} p_{\mathcal{I}}\log\frac{|\det\mathsf{H}_{\mathcal{I}}|}{\mathsf{V}_{\mathsf{H}}} + \log\mathsf{V}_{\mathsf{H}} + n_{\mathrm{R}}\log\mathsf{A} \\
&\quad + n_{\mathrm{R}}\bigg(1 - \log\frac{\mu}{1-e^{-\mu}} - \frac{\mu\, e^{-\mu}}{1-e^{-\mu}}\bigg) &(172)\\
&= -\mathsf{D}(\mathbf{p}\|\mathbf{q}) + \log\mathsf{V}_{\mathsf{H}} + n_{\mathrm{R}}\log\mathsf{A} + n_{\mathrm{R}}\bigg(1 - \log\frac{\mu}{1-e^{-\mu}} - \frac{\mu\, e^{-\mu}}{1-e^{-\mu}}\bigg). &(173)
\end{aligned}$$

Here, (169) holds because $\mathsf{H}(U|\bar{\mathbf{X}}) = 0$; (171) follows from the differential entropy of a truncated exponential distribution; and in (173) we used the definition of $\mathbf{q}$ in (57). Then, (67) follows by plugging (173) into (150).

E Derivation of Upper Bounds

Let $\bar{\mathbf{X}}^\star$ be a maximizer in (38) and let $U^\star$ be defined by $\bar{\mathbf{X}}^\star$ as in (40). Then,

$$\begin{aligned}
\mathsf{C}_{\mathsf{H}}(\mathsf{A},\alpha\mathsf{A}) &= \mathrm{I}\big(\bar{\mathbf{X}}^\star;\bar{\mathbf{X}}^\star + \mathbf{Z}\big) &(174)\\
&\le \mathrm{I}\big(\bar{\mathbf{X}}^\star;\bar{\mathbf{X}}^\star + \mathbf{Z}, U^\star\big) &(175)
\end{aligned}$$

$$\leq \mathsf{H}(U^\star) + \mathsf{I}\big(\bar{\mathbf{X}}^\star; \bar{\mathbf{X}}^\star + \mathbf{Z}\big|U^\star\big). \tag{176}$$

For each set $\mathcal{I} \in \mathcal{U}$, we have

$$\begin{aligned}
\mathsf{I}\big(\bar{\mathbf{X}}^\star; \bar{\mathbf{X}}^\star + \mathbf{Z}\big|U^\star = \mathcal{I}\big) &= \mathsf{I}\big(\bar{\mathbf{X}}^\star - \mathbf{v}_\mathcal{I}; (\bar{\mathbf{X}}^\star - \mathbf{v}_\mathcal{I}) + \mathbf{Z}\big|U^\star = \mathcal{I}\big) && (177)\\
&= \mathsf{I}\big(\mathsf{H}_\mathcal{I}^{-1}(\bar{\mathbf{X}}^\star - \mathbf{v}_\mathcal{I}); \mathsf{H}_\mathcal{I}^{-1}(\bar{\mathbf{X}}^\star - \mathbf{v}_\mathcal{I}) + \mathsf{H}_\mathcal{I}^{-1}\mathbf{Z}\big|U^\star = \mathcal{I}\big) && (178)\\
&= \mathsf{I}(\mathbf{X}_\mathcal{I}; \mathbf{X}_\mathcal{I} + \mathbf{Z}_\mathcal{I}|U^\star = \mathcal{I}) && (179)
\end{aligned}$$

where we have defined

$$\mathbf{Z}_\mathcal{I} \triangleq \mathsf{H}_\mathcal{I}^{-1}\mathbf{Z}, \tag{180}$$

$$\mathbf{X}_\mathcal{I} \triangleq \mathsf{H}_\mathcal{I}^{-1}(\mathbf{X}^\star - \mathbf{v}_\mathcal{I}). \tag{181}$$

It should be noted that

$$\mathbf{Z}_\mathcal{I} \sim \mathcal{N}\big(0, \mathsf{H}_\mathcal{I}^{-1}\mathsf{H}_\mathcal{I}^{-\mathsf{T}}\big). \tag{182}$$

Moreover, $\mathbf{X}_\mathcal{I}$ is subject to the following peak- and average-power constraints:

$$\Pr\big[\bar{X}_{\mathcal{I},\ell} > \mathsf{A}\big] = 0, \quad \forall\, \ell \in \{1, \ldots, n_\mathrm{R}\}, \tag{183a}$$

$$\mathsf{E}\big[\|\mathbf{X}_\mathcal{I}\|_1\big] = \mathsf{E}_\mathcal{I}, \tag{183b}$$

where the set $\{\mathsf{E}_\mathcal{I} \colon \mathcal{I} \in \mathcal{U}\}$ satisfies

$$\sum_{\mathcal{I}\in\mathcal{U}} p_\mathcal{I}(s_\mathcal{I}\mathsf{A} + \mathsf{E}_\mathcal{I}) \leq \alpha\mathsf{A}. \tag{184}$$

To further bound the RHS of (179), we use the duality-based upper-bounding technique using a product output distribution

$$R_\mathcal{I}(\mathbf{y}_\mathcal{I}) = \prod_{\ell=1}^{n_\mathrm{R}} R_{\mathcal{I},\ell}(y_{\mathcal{I},\ell}). \tag{185}$$

Denoting by $W_\mathcal{I}(\cdot|\mathbf{X}_\mathcal{I})$ the transition law of the $n_\mathrm{R} \times n_\mathrm{R}$ MIMO channel with input $\mathbf{X}_\mathcal{I}$ and output $\mathbf{Y}_\mathcal{I} \triangleq \mathbf{X}_\mathcal{I} + \mathbf{Z}_\mathcal{I}$, and by $W_{\mathcal{I},\ell}(\cdot|\bar{X}_{\mathcal{I},\ell})$ the marginal transition law of its ℓth component, we have:

$$\begin{aligned}
&\mathsf{I}(\mathbf{X}_\mathcal{I}; \mathbf{X}_\mathcal{I} + \mathbf{Z}_\mathcal{I}|U^\star = \mathcal{I})\\
&\quad\leq \mathsf{E}_{\mathbf{X}_\mathcal{I}|U^\star=\mathcal{I}}\big[\mathsf{D}\big(W_\mathcal{I}(\cdot|\mathbf{X}_\mathcal{I})\big\|R_\mathcal{I}(\cdot)\big)\big] && (186)\\
&\quad= -\,\mathsf{h}\big(\mathbf{X}_\mathcal{I} + \mathbf{Z}_\mathcal{I}\big|\mathbf{X}_\mathcal{I}, U^\star = \mathcal{I}\big) - \mathsf{E}_{\mathbf{X}_\mathcal{I}|U^\star=\mathcal{I}}\left[\sum_{\ell=1}^{n_\mathrm{R}} \mathsf{E}_{W_\mathcal{I}(\mathbf{Y}_\mathcal{I}|\mathbf{X}_\mathcal{I})}[\log R_{\mathcal{I},\ell}(Y_{\mathcal{I},\ell})]\right] && (187)\\
&\quad= -\frac{n_\mathrm{R}}{2}\log 2\pi e + \log|\det \mathsf{H}_\mathcal{I}| - \sum_{\ell=1}^{n_\mathrm{R}} \mathsf{E}_{\bar{X}_{\mathcal{I},\ell}|U^\star=\mathcal{I}}\Big[\mathsf{E}_{W_{\mathcal{I},\ell}(Y_{\mathcal{I},\ell}|\bar{X}_{\mathcal{I},\ell})}[\log R_{\mathcal{I},\ell}(Y_{\mathcal{I},\ell})]\Big], && (188)
\end{aligned}$$

where the last equality holds because

$$\mathsf{h}(\mathbf{X}_\mathcal{I} + \mathbf{Z}_\mathcal{I}|\mathbf{X}_\mathcal{I}, U^\star = \mathcal{I}) = \mathsf{h}(\mathbf{Z}_\mathcal{I}) = \frac{1}{2}\log\big((2\pi e)^{n_\mathrm{R}} \det \mathsf{H}_\mathcal{I}^{-1}\mathsf{H}_\mathcal{I}^{-\mathsf{T}}\big). \tag{189}$$

We finally combine (176) with (179) and (188) to obtain

$$\begin{aligned}
\mathsf{C_H}(\mathsf{A}, \alpha\mathsf{A}) \leq \mathsf{H}(\mathbf{p}^*) &- \sum_{\ell=1}^{n_\mathrm{R}}\sum_{\mathcal{I}\in\mathcal{U}} p_\mathcal{I}^*\, \mathsf{E}_{\bar{X}_{\mathcal{I},\ell}|U^\star=\mathcal{I}}\Big[\mathsf{E}_{W_{\mathcal{I},\ell}(Y_{\mathcal{I},\ell}|\bar{X}_{\mathcal{I},\ell})}[\log R_{\mathcal{I},\ell}(Y_{\mathcal{I},\ell})]\Big]\\
&+ \sum_{\mathcal{I}\in\mathcal{U}} p_\mathcal{I}^* \log|\det \mathsf{H}_\mathcal{I}| - \frac{n_\mathrm{R}}{2}\log 2\pi e, && (190)
\end{aligned}$$

where $\mathbf{p}^*$ denotes the probability vector of $U^\star$. The bounds in Section 6.2 are then found by picking appropriate choices for the distribution on the output alphabet $R_{\mathcal{I},\ell}(\cdot)$. We elaborate on this in the following.

E.1 Proof of Theorem 16

Inspired by [6] and [7], we choose

$$R_{\mathcal{I},\ell}(y) = \begin{cases} \frac{\beta}{\sqrt{2\pi}\sigma_{\mathcal{I},\ell}} \cdot e^{-\frac{y^2}{2\sigma_{\mathcal{I},\ell}^2}} & \text{if } y \in (-\infty, 0), \\ (1-\beta) \cdot \frac{1}{\mathsf{A}} & \text{if } y \in [0, \mathsf{A}], \\ \frac{\beta}{\sqrt{2\pi}\sigma_{\mathcal{I},\ell}} \cdot e^{-\frac{(y-\mathsf{A})^2}{2\sigma_{\mathcal{I},\ell}^2}} & \text{if } y \in (\mathsf{A}, \infty), \end{cases} \tag{191}$$

where $\beta \in (0,1)$ will be specified later. Recall that $\sigma_{\mathcal{I},\ell}$ is the square root of the ℓth diagonal entry of the matrix $\mathsf{H}_{\mathcal{I}}^{-1}\mathsf{H}_{\mathcal{I}}^{-\mathsf{T}}$, i.e.,

$$\sigma_{\mathcal{I},\ell} = \sqrt{\mathsf{Var}[Z_{\mathcal{I},\ell}]}. \tag{192}$$

We notice that

$$\begin{aligned} &-\int_{-\infty}^{0} W_{\mathcal{I},\ell}(y|x) \log R_{\mathcal{I},\ell}(y)\,\mathrm{d}y \\ &= -\int_{-\infty}^{0} \frac{1}{\sqrt{2\pi}\sigma_{\mathcal{I},\ell}}\, e^{-\frac{(y-x)^2}{2\sigma_{\mathcal{I},\ell}^2}} \left(\log \frac{\beta}{\sqrt{2\pi}\sigma_{\mathcal{I},\ell}} - \frac{y^2}{2\sigma_{\mathcal{I},\ell}^2} \right) \mathrm{d}y \qquad (193) \\ &= -\log\left(\frac{\beta}{\sqrt{2\pi}\sigma_{\mathcal{I},\ell}} \right) \mathcal{Q}\left(\frac{x}{\sigma_{\mathcal{I},\ell}} \right) + \frac{1}{2}\,\mathcal{Q}\left(\frac{x}{\sigma_{\mathcal{I},\ell}} \right) \\ &\quad + \frac{1}{2}\left(\frac{x}{\sigma_{\mathcal{I},\ell}} \right)^2 \mathcal{Q}\left(\frac{x}{\sigma_{\mathcal{I},\ell}} \right) - \frac{x}{2\sigma_{\mathcal{I},\ell}}\phi\left(\frac{x}{\sigma_{\mathcal{I},\ell}} \right) \qquad (194) \\ &\le -\left(\log \frac{\beta}{\sqrt{2\pi}\sigma_{\mathcal{I},\ell}} - \frac{1}{2} \right) \mathcal{Q}\left(\frac{x}{\sigma_{\mathcal{I},\ell}} \right) \qquad (195) \\ &= -\log \frac{\beta}{\sqrt{2\pi e}\sigma_{\mathcal{I},\ell}} \cdot \mathcal{Q}\left(\frac{x}{\sigma_{\mathcal{I},\ell}} \right), \qquad (196) \end{aligned}$$

where

$$\phi(x) \triangleq \frac{1}{\sqrt{2\pi}}\, e^{-\frac{x^2}{2}}, \tag{197}$$

and where (195) holds because of [26, Prop. A.8]

$$\xi\mathcal{Q}(\xi) \le \phi(\xi), \quad \xi \ge 0. \tag{198}$$

Similarly,

$$-\int_{\mathsf{A}}^{\infty} W_{\mathcal{I},\ell}(y|x) \log R_{\mathcal{I},\ell}(y)\,\mathrm{d}y \le -\log \frac{\beta}{\sqrt{2\pi e}\sigma_{\mathcal{I},\ell}} \cdot \mathcal{Q}\left(\frac{\mathsf{A}-x}{\sigma_{\mathcal{I},\ell}} \right). \tag{199}$$

Moreover, we have

$$\begin{aligned} -\int_{0}^{\mathsf{A}} W_{\mathcal{I},\ell}(y|x) \log R_{\mathcal{I},\ell}(y)\,\mathrm{d}y &= -\int_{0}^{\mathsf{A}} \frac{1}{\sqrt{2\pi}\sigma_{\mathcal{I},\ell}}\, e^{-\frac{(y-x)^2}{2\sigma_{\mathcal{I},\ell}^2}} \log \frac{(1-\beta)}{\mathsf{A}}\,\mathrm{d}y \qquad (200) \\ &= \log\left(\frac{\mathsf{A}}{1-\beta} \right) \cdot \left(1 - \mathcal{Q}\left(\frac{x}{\sigma_{\mathcal{I},\ell}} \right) - \mathcal{Q}\left(\frac{\mathsf{A}-x}{\sigma_{\mathcal{I},\ell}} \right) \right). \qquad (201) \end{aligned}$$

We choose

$$\beta = \frac{\sqrt{2\pi e}\sigma_{\mathcal{I},\ell}}{\mathsf{A} + \sqrt{2\pi e}\sigma_{\mathcal{I},\ell}} \tag{202}$$

and obtain from (196), (199), and (201)

$$-\mathsf{E}_{W_{\mathcal{I},\ell}(Y_{\mathcal{I},\ell}|\bar{X}_{\mathcal{I},\ell})}[\log R_{\mathcal{I},\ell}(Y_{\mathcal{I},\ell})] \leq \log\bigl(\mathsf{A} + \sqrt{2\pi e}\sigma_{\mathcal{I},\ell}\bigr). \tag{203}$$

Substituting (203) into (190) then yields

$$\begin{aligned}
\mathsf{C}_{\mathsf{H}}(\mathsf{A}, \alpha\mathsf{A}) &\leq \sup_{\mathbf{p}}\Biggl\{\mathsf{H}(\mathbf{p}) - \frac{n_{\mathrm{R}}}{2}\log 2\pi e + \sum_{\mathcal{I}\in\mathcal{U}} p_{\mathcal{I}}\log|\det\mathsf{H}_{\mathcal{I}}| \\
&\qquad + \sum_{\mathcal{I}\in\mathcal{U}} p_{\mathcal{I}}\sum_{\ell=1}^{n_{\mathrm{R}}}\log\Bigl(\mathsf{A} + \sqrt{2\pi e}\sigma_{\mathcal{I},\ell}\Bigr)\Biggr\} && (204)\\
&= \sup_{\mathbf{p}}\Biggl\{\mathsf{H}(\mathbf{p}) + \sum_{\mathcal{I}\in\mathcal{U}} p_{\mathcal{I}}\log\frac{|\det\mathsf{H}_{\mathcal{I}}|}{\mathsf{V}_{\mathsf{H}}} + \log\mathsf{V}_{\mathsf{H}} \\
&\qquad + \sum_{\mathcal{I}\in\mathcal{U}} p_{\mathcal{I}}\sum_{\ell=1}^{n_{\mathrm{R}}}\log\biggl(\sigma_{\mathcal{I},\ell} + \frac{\mathsf{A}}{\sqrt{2\pi e}}\biggr)\Biggr\} && (205)\\
&= \sup_{\mathbf{p}}\Biggl\{\log\mathsf{V}_{\mathsf{H}} - \mathsf{D}(\mathbf{p}\|\mathbf{q}) + \sum_{\mathcal{I}\in\mathcal{U}} p_{\mathcal{I}}\sum_{\ell=1}^{n_{\mathrm{R}}}\log\biggl(\sigma_{\mathcal{I},\ell} + \frac{\mathsf{A}}{\sqrt{2\pi e}}\biggr)\Biggr\}. && (206)
\end{aligned}$$

E.2 Proof of Theorem 17

We choose

$$R_{\mathcal{I},\ell}(y) = \begin{cases} \frac{\beta}{\sqrt{2\pi}\sigma_{\mathcal{I},\ell}}\, e^{-\frac{y^2}{2\sigma_{\mathcal{I},\ell}^2}} & \text{if } y \in (-\infty, 0), \\ \frac{1-\beta}{\mathsf{A}}\cdot\frac{\mu}{1-e^{-\mu}}\, e^{-\frac{\mu y}{\mathsf{A}}} & \text{if } y \in [0, \mathsf{A}], \\ \frac{\beta}{\sqrt{2\pi}\sigma_{\mathcal{I},\ell}}\, e^{-\frac{(y-\mathsf{A})^2}{2\sigma_{\mathcal{I},\ell}^2}} & \text{if } y \in (\mathsf{A}, \infty), \end{cases} \tag{207}$$

where $\beta \in (0,1)$ and $\mu > 0$ will be specified later.

We notice that the inequalities in (196) and (199) still hold, while

$$\begin{aligned}
&-\int_0^{\mathsf{A}} W_{\mathcal{I},\ell}(y|x)\log R_{\mathcal{I},\ell}(y)\,\mathrm{d}y \\
&= -\int_0^{\mathsf{A}} \frac{1}{\sqrt{2\pi}\sigma_{\mathcal{I},\ell}}\, e^{-\frac{(y-x)^2}{2\sigma_{\mathcal{I},\ell}^2}}\biggl(\log\frac{1-\beta}{\mathsf{A}}\frac{\mu}{1-e^{-\mu}} - \frac{\mu}{\mathsf{A}}y\biggr)\mathrm{d}y && (208)\\
&= -\log\biggl(\frac{1-\beta}{\mathsf{A}}\frac{\mu}{1-e^{-\mu}}\biggr)\biggl(1 - \mathcal{Q}\biggl(\frac{x}{\sigma_{\mathcal{I},\ell}}\biggr) - \mathcal{Q}\biggl(\frac{\mathsf{A}-x}{\sigma_{\mathcal{I},\ell}}\biggr)\biggr) \\
&\quad + \frac{\mu\sigma_{\mathcal{I},\ell}}{\mathsf{A}}\biggl(\phi\biggl(\frac{x}{\sigma_{\mathcal{I},\ell}}\biggr) - \phi\biggl(\frac{\mathsf{A}-x}{\sigma_{\mathcal{I},\ell}}\biggr)\biggr) + \frac{\mu}{\mathsf{A}}x\biggl(1 - \mathcal{Q}\biggl(\frac{x}{\sigma_{\mathcal{I},\ell}}\biggr) - \mathcal{Q}\biggl(\frac{\mathsf{A}-x}{\sigma_{\mathcal{I},\ell}}\biggr)\biggr) && (209)\\
&\leq -\log\biggl(\frac{1-\beta}{\mathsf{A}}\frac{\mu}{1-e^{-\mu}}\biggr)\biggl(1 - \mathcal{Q}\biggl(\frac{x}{\sigma_{\mathcal{I},\ell}}\biggr) - \mathcal{Q}\biggl(\frac{\mathsf{A}-x}{\sigma_{\mathcal{I},\ell}}\biggr)\biggr) \\
&\quad + \frac{\mu\sigma_{\mathcal{I},\ell}}{\mathsf{A}}\biggl(\phi(0) - \phi\biggl(\frac{\mathsf{A}}{\sigma_{\mathcal{I},\ell}}\biggr)\biggr) + \frac{\mu}{\mathsf{A}}x\biggl(1 - 2\,\mathcal{Q}\biggl(\frac{\mathsf{A}}{2\sigma_{\mathcal{I},\ell}}\biggr)\biggr) && (210)\\
&\leq -\log\biggl(\frac{1-\beta}{\mathsf{A}}\frac{\mu}{1-e^{-\mu}}\biggr)\biggl(1 - \mathcal{Q}\biggl(\frac{x}{\sigma_{\mathcal{I},\ell}}\biggr) - \mathcal{Q}\biggl(\frac{\mathsf{A}-x}{\sigma_{\mathcal{I},\ell}}\biggr)\biggr) \\
&\quad + \frac{\mu\sigma_{\mathcal{I},\ell}}{\mathsf{A}}\biggl(\phi(0) - \phi\biggl(\frac{\mathsf{A}}{\sigma_{\mathcal{I},\ell}}\biggr)\biggr) + \frac{\mu}{\mathsf{A}}x. && (211)
\end{aligned}$$

Here (210) follows from the fact that, for $\xi \in [0, \mathsf{A}]$, $1 - \mathcal{Q}(\xi) - \mathcal{Q}(\mathsf{A} - \xi)$ achieves the maximum value at $\xi = \frac{\mathsf{A}}{2}$, and that $\phi(\xi)$ is monotonically decreasing; and (211) holds because $1 - 2\,\mathcal{Q}(\xi) \leq 1$ and because $x \geq 0$.

Combining (196), (199), and (211), and choosing

$$\beta = \frac{\mu\sqrt{2\pi e}\sigma_{\mathcal{I},\ell}}{\mathsf{A}(1-e^{-\mu}) + \mu\sqrt{2\pi e}\sigma_{\mathcal{I},\ell}} \tag{212}$$

now yield

$$\begin{aligned} &-\mathsf{E}_{W_{\mathcal{I},\ell}(Y_{\mathcal{I},\ell}|\bar{x}_{\mathcal{I},\ell})}[\log R_{\mathcal{I},\ell}(Y_{\mathcal{I},\ell})] \\ &\quad\le \log\left(\sqrt{2\pi e}\sigma_{\mathcal{I},\ell} + \mathsf{A}\cdot\frac{1-e^{-\mu}}{\mu}\right) + \frac{\mu\sigma_{\mathcal{I},\ell}}{\mathsf{A}\sqrt{2\pi}}\left(1-e^{-\frac{\mathsf{A}^2}{2\sigma^2_{\mathcal{I},\ell}}}\right) + \frac{\mu}{\mathsf{A}}\bar{x}_{\mathcal{I},\ell}. \end{aligned} \tag{213}$$

Substituting (213) into (190), we have

$$\begin{aligned} &\mathsf{C_H}(\mathsf{A},\alpha\mathsf{A}) \\ &\le \mathsf{H}(\mathbf{p}^*) + \sum_{\mathcal{I}\in\mathcal{U}} p^*_{\mathcal{I}}\log|\det \mathsf{H}_{\mathcal{I}}| - \frac{n_{\mathrm{R}}}{2}\log 2\pi e + \sum_{\mathcal{I}\in\mathcal{U}} p^*_{\mathcal{I}}\sum_{\ell=1}^{n_{\mathrm{R}}}\log\left(\sqrt{2\pi e}\sigma_{\mathcal{I},\ell} + \mathsf{A}\cdot\frac{1-e^{-\mu}}{\mu}\right) \\ &\quad + \frac{\mu}{\mathsf{A}\sqrt{2\pi}}\sum_{\mathcal{I}\in\mathcal{U}} p^*_{\mathcal{I}}\sum_{\ell=1}^{n_{\mathrm{R}}}\sigma_{\mathcal{I},\ell}\left(1-e^{-\frac{\mathsf{A}^2}{2\sigma^2_{\mathcal{I},\ell}}}\right) + \frac{\mu}{\mathsf{A}}\sum_{\mathcal{I}\in\mathcal{U}} p^*_{\mathcal{I}}\sum_{\ell=1}^{n_{\mathrm{R}}}\mathsf{E}\left[\bar{X}_{\mathcal{I},\ell}\,\middle|\,U^\star=\mathcal{I}\right] \quad (214) \\ &= \mathsf{H}(\mathbf{p}^*) + \sum_{\mathcal{I}\in\mathcal{U}} p^*_{\mathcal{I}}\log\frac{|\det \mathsf{H}_{\mathcal{I}}|}{\mathsf{V_H}} + \log\mathsf{V_H} + \sum_{\mathcal{I}\in\mathcal{U}} p^*_{\mathcal{I}}\sum_{\ell=1}^{n_{\mathrm{R}}}\log\left(\sigma_{\mathcal{I},\ell} + \frac{\mathsf{A}}{\sqrt{2\pi e}}\cdot\frac{1-e^{-\mu}}{\mu}\right) \\ &\quad + \frac{\mu}{\mathsf{A}\sqrt{2\pi}}\sum_{\mathcal{I}\in\mathcal{U}} p^*_{\mathcal{I}}\sum_{\ell=1}^{n_{\mathrm{R}}}\sigma_{\mathcal{I},\ell}\left(1-e^{-\frac{\mathsf{A}^2}{2\sigma^2_{\mathcal{I},\ell}}}\right) + \frac{\mu}{\mathsf{A}}\sum_{\mathcal{I}\in\mathcal{U}} p^*_{\mathcal{I}}\left\|\mathsf{H}_{\mathcal{I}}^{-1}\left(\mathsf{E}[\mathbf{X}^\star\,|\,U^\star=\mathcal{I}] - \mathbf{v}_{\mathcal{I}}\right)\right\|_1 \\ &\qquad\qquad (215) \\ &\le \log\mathsf{V_H} - \mathsf{D}(\mathbf{p}^*\|\mathbf{q}) + \sum_{\mathcal{I}\in\mathcal{U}} p^*_{\mathcal{I}}\sum_{\ell=1}^{n_{\mathrm{R}}}\log\left(\sigma_{\mathcal{I},\ell} + \frac{\mathsf{A}}{\sqrt{2\pi e}}\cdot\frac{1-e^{-\mu}}{\mu}\right) \\ &\quad + \frac{\mu}{\mathsf{A}\sqrt{2\pi}}\sum_{\mathcal{I}\in\mathcal{U}} p^*_{\mathcal{I}}\sum_{\ell=1}^{n_{\mathrm{R}}}\sigma_{\mathcal{I},\ell}\left(1-e^{-\frac{\mathsf{A}^2}{2\sigma^2_{\mathcal{I},\ell}}}\right) + \mu\left(\alpha - \sum_{\mathcal{I}\in\mathcal{U}} p^*_{\mathcal{I}}s_{\mathcal{I}}\right), \quad (216) \end{aligned}$$

where (215) follows from (181), and (216) from (39). Theorem 17 is proven by taking the supremum over the probability vector $\mathbf{p}$ and the infimum over $\mu > 0$.

E.3 Proof of Theorem 18

We choose

$$R_{\mathcal{I},\ell}(y) = \begin{cases} \frac{1}{\sqrt{2\pi}\sigma_{\mathcal{I},\ell}}\, e^{-\frac{y^2}{2\sigma^2_{\mathcal{I},\ell}}} & \text{if } y\in(-\infty,-\delta), \\ \frac{\mu}{\mathsf{A}}\cdot\frac{1-2\,\mathcal{Q}\left(\frac{\delta}{\sigma_{\mathcal{I},\ell}}\right)}{e^{\frac{\mu\delta}{\mathsf{A}}} - e^{-\mu(1+\frac{\delta}{\mathsf{A}})}}\, e^{-\frac{\mu y}{\mathsf{A}}} & \text{if } y\in[-\delta,\mathsf{A}+\delta], \\ \frac{1}{\sqrt{2\pi}\sigma_{\mathcal{I},\ell}}\, e^{-\frac{(y-\mathsf{A})^2}{2\sigma^2_{\mathcal{I},\ell}}} & \text{if } y\in(\mathsf{A}+\delta,\infty), \end{cases} \tag{217}$$

where $\delta,\mu > 0$ are free parameters. Following the steps in the proof of [5, App. B.B] and bounding $1-\mathcal{Q}(\xi_1)-\mathcal{Q}(\xi_2)\le 1$, we obtain:

$$\begin{aligned} &-\mathsf{E}_{\bar{X}_{\mathcal{I},\ell}|U^\star=\mathcal{I}}\Big[\mathsf{E}_{W_{\mathcal{I},\ell}(Y_{\mathcal{I},\ell}|\bar{X}_{\mathcal{I},\ell})}[\log R_{\mathcal{I},\ell}(Y_{\mathcal{I},\ell})]\Big] \\ &\quad\le \log\left(\mathsf{A}\cdot\frac{e^{\frac{\mu\delta}{\mathsf{A}}} - e^{-\mu(1+\frac{\delta}{\mathsf{A}})}}{\mu\left(1-2\,\mathcal{Q}\left(\frac{\delta}{\sigma_{\mathcal{I},\ell}}\right)\right)}\right) + \frac{\delta}{\sqrt{2\pi}\sigma_{\mathcal{I},\ell}}\,e^{-\frac{\delta^2}{2\sigma^2_{\mathcal{I},\ell}}} + \mathcal{Q}\left(\frac{\delta}{\sigma_{\mathcal{I},\ell}}\right) \\ &\qquad + \frac{\mu\sigma_{\mathcal{I},\ell}}{\mathsf{A}\sqrt{2\pi}}\left(e^{-\frac{\delta^2}{2\sigma^2_{\mathcal{I},\ell}}} - e^{-\frac{(\mathsf{A}+\delta)^2}{2\sigma^2_{\mathcal{I},\ell}}}\right) + \frac{\mu}{\mathsf{A}}\,\mathsf{E}\left[\bar{X}_{\mathcal{I},\ell}\,\middle|\,U^\star=\mathcal{I}\right]. \end{aligned} \tag{218}$$

Plugging (218) into (190) and using a derivation analogous to (214)–(216) then results in the given bound.

E.4 Proof of Theorem 19

Using that

$$\mathsf{h}(\mathbf{Y}) \le \frac{1}{2}\log\bigl((2\pi e)^{n_{\mathrm{R}}}\det \mathsf{K}_{\mathbf{YY}}\bigr), \tag{219}$$

where

$$\mathsf{K}_{\mathbf{YY}} = \mathsf{K}_{\bar{\mathbf{X}}\bar{\mathbf{X}}} + \mathsf{I}, \tag{220}$$

we have

$$\begin{aligned}
\mathsf{C_H}(\mathsf{A}, \alpha\mathsf{A}) &= \max_{P_{\mathbf{X}}} \bigl\{\mathsf{h}(\mathbf{Y}) - \mathsf{h}(\mathbf{Z})\bigr\} &(221)\\
&\le \max_{P_{\mathbf{X}}} \left\{\frac{1}{2}\log\bigl((2\pi e)^{n_{\mathrm{R}}}\det(\mathsf{K}_{\bar{\mathbf{X}}\bar{\mathbf{X}}} + \mathsf{I})\bigr) - \frac{1}{2}\log(2\pi e)^{n_{\mathrm{R}}}\right\} &(222)\\
&= \max_{P_{\mathbf{X}}} \frac{1}{2}\log\det(\mathsf{I} + \mathsf{K}_{\bar{\mathbf{X}}\bar{\mathbf{X}}}) &(223)\\
&\le \max_{P_{\mathbf{X}}} \frac{1}{2}\log\prod_{i=1}^{n_{\mathrm{R}}}\bigl(\mathsf{I} + \mathsf{K}_{\bar{\mathbf{X}}\bar{\mathbf{X}}}\bigr)_{i,i} &(224)\\
&= \max_{P_{\mathbf{X}}} \frac{n_{\mathrm{R}}}{2}\sum_{i=1}^{n_{\mathrm{R}}}\frac{1}{n_{\mathrm{R}}}\log\Bigl(1 + \bigl(\mathsf{K}_{\bar{\mathbf{X}}\bar{\mathbf{X}}}\bigr)_{i,i}\Bigr) &(225)\\
&\le \max_{P_{\mathbf{X}}} \frac{n_{\mathrm{R}}}{2}\log\left(1 + \sum_{i=1}^{n_{\mathrm{R}}}\frac{1}{n_{\mathrm{R}}}\bigl(\mathsf{K}_{\bar{\mathbf{X}}\bar{\mathbf{X}}}\bigr)_{i,i}\right) &(226)\\
&= \max_{P_{\mathbf{X}}} \frac{n_{\mathrm{R}}}{2}\log\left(1 + \frac{1}{n_{\mathrm{R}}}\operatorname{tr}\bigl(\mathsf{K}_{\bar{\mathbf{X}}\bar{\mathbf{X}}}\bigr)\right) &(227)\\
&= \frac{n_{\mathrm{R}}}{2}\log\left(1 + \frac{1}{n_{\mathrm{R}}}\max_{P_{\mathbf{X}}}\operatorname{tr}\bigl(\mathsf{K}_{\bar{\mathbf{X}}\bar{\mathbf{X}}}\bigr)\right). &(228)
\end{aligned}$$

Here, (224) follows from Hadamard's inequality, and (226) follows from Jensen's inequality.

F Derivation of Asymptotic Results

F.1 Proof of Theorem 20

It follows directly from Theorem 14 that the RHS of (76) is a lower bound to its LHS. To prove the other direction, using that $\mathsf{D}(\mathbf{p}\|\mathbf{q}) \ge 0$, we have from Theorem 16 that

$$\mathsf{C_H}(\mathsf{A}, \alpha\mathsf{A}) \le \log \mathsf{V_H} + n_{\mathrm{R}}\log\left(\sigma_{\max} + \frac{\mathsf{A}}{\sqrt{2\pi e}}\right) \tag{229}$$

where

$$\sigma_{\max} \triangleq \max_{\substack{\mathcal{I}\in\mathcal{U}\\ \ell\in\{1,\ldots,n_{\mathrm{R}}\}}} \sigma_{\mathcal{I},\ell}. \tag{230}$$

This proves that the RHS of (76) is also an upper bound to its LHS, and hence completes the proof of (76).

Next, we prove (77). Again, that its RHS is a lower bound to its LHS follows immediately from Theorem 15. To prove the other direction, we define for any $\mathbf{p}$:

$$\lambda(\mathbf{p}) \triangleq \alpha - \sum_{\mathcal{I}\in\mathcal{U}} p_{\mathcal{I}} s_{\mathcal{I}} \le \alpha. \tag{231}$$

We then fix $\mathsf{A} \geq 1$ and choose μ depending on $\lambda(\mathbf{p})$ to be

$$\mu = \begin{cases} \mu^*(\mathbf{p}) & \text{if } \mathsf{A}^{-(1-\zeta)} < \frac{\lambda(\mathbf{p})}{n_\mathrm{R}} < \frac{1}{2}, \\ \mathsf{A}^{1-\zeta} & \text{if } \frac{\lambda(\mathbf{p})}{n_\mathrm{R}} \leq \mathsf{A}^{-(1-\zeta)}, \\ \frac{1}{\mathsf{A}} & \text{if } \frac{\lambda(\mathbf{p})}{n_\mathrm{R}} \geq \frac{1}{2}, \end{cases} \tag{232}$$

where $0 < \zeta < 1$ is a free parameter and $\mu^*(\mathbf{p})$ is the unique solution to

$$\frac{1}{\mu^*} - \frac{e^{-\mu^*}}{1 - e^{-\mu^*}} = \frac{\lambda(\mathbf{p})}{n_\mathrm{R}}. \tag{233}$$

Note that in the first case of (232),

$$\mathsf{A}^{-(1-\zeta)} < \frac{\lambda(\mathbf{p})}{n_\mathrm{R}} = \frac{1}{\mu^*(\mathbf{p})} - \frac{e^{-\mu^*(\mathbf{p})}}{1 - e^{-\mu^*(\mathbf{p})}} < \frac{1}{\mu^*(\mathbf{p})}, \tag{234}$$

i.e.,

$$\mu^*(\mathbf{p}) < \mathsf{A}^{1-\zeta}, \tag{235}$$

and thus the choice (232) makes sure that in all three cases, irrespective of $\mathbf{p}$:

$$\mu \leq \mathsf{A}^{1-\zeta}, \quad \text{for } \mathsf{A} \geq 1. \tag{236}$$

Then, for $\mathsf{A} \geq 1$, the upper bound (72) can be loosened as follows:

$$\mathsf{C}_\mathsf{H}(\mathsf{A}, \alpha\mathsf{A}) \leq \frac{1}{2} \log\left(\frac{\mathsf{A}^{2n_\mathrm{R}} \mathsf{V}_\mathsf{H}^2}{(2\pi e)^{n_\mathrm{R}}}\right) + f(\mathsf{A}) + \sup_{\mathbf{p}} g(\mathsf{A}, \mathbf{p}, \mu) \tag{237}$$

where

$$f(\mathsf{A}) \triangleq \frac{n_\mathrm{R} \sigma_{\max}}{\mathsf{A}^\zeta \sqrt{2\pi}} \left(1 - e^{-\frac{\mathsf{A}^2}{2\sigma_{\min}^2}}\right), \tag{238}$$

$$g(\mathsf{A}, \mathbf{p}, \mu) \triangleq n_\mathrm{R} \log\left(\frac{\sqrt{2\pi e}\sigma_{\max}}{\mathsf{A}} + \frac{1 - e^{-\mu}}{\mu}\right) + \mu\lambda(\mathbf{p}) - \mathsf{D}(\mathbf{p}\|\mathbf{q}) \tag{239}$$

with $\sigma_{\max}$ defined in (230) and with

$$\sigma_{\min} \triangleq \min_{\substack{\mathcal{I} \in \mathcal{U} \\ \ell \in \{1, \ldots, n_\mathrm{R}\}}} \sigma_{\mathcal{I},\ell}. \tag{240}$$

Note that

$$\lim_{\mathsf{A} \to \infty} f(\mathsf{A}) = 0. \tag{241}$$

Next, we upper-bound $g(\mathsf{A}, \mathbf{p}, \mu)$ individually for each of the three different cases in (232) to obtain a bound of the form

$$g(\mathsf{A}, \mathbf{p}, \mu) \leq \begin{cases} g_1(\mathsf{A}) & \text{if } \mathsf{A}^{-(1-\zeta)} < \frac{\lambda(\mathbf{p})}{n_\mathrm{R}} < \frac{1}{2}, \\ g_2(\mathsf{A}) & \text{if } \frac{\lambda(\mathbf{p})}{n_\mathrm{R}} \leq \mathsf{A}^{-(1-\zeta)}, \\ g_3(\mathsf{A}) & \text{if } \frac{\lambda(\mathbf{p})}{n_\mathrm{R}} \geq \frac{1}{2}, \end{cases} \tag{242}$$

for three functions g_1, g_2, and g_3 that only depend on A but not on $\mathbf{p}$ or μ. Thus, we shall then obtain the bound

$$g(\mathsf{A}, \mathbf{p}, \mu) \leq \max\{g_1(\mathsf{A}), g_2(\mathsf{A}), g_3(\mathsf{A})\}, \quad \mathsf{A} \geq 1. \tag{243}$$

The functions g_1, g_2, and g_3 are introduced in the following.

For the first case where $\frac{\lambda(\mathbf{p})}{n_\mathrm{R}} \in \bigl(\mathsf{A}^{-(1-\zeta)}, \frac{1}{2}\bigr)$, we have

$$\begin{aligned} g(\mathsf{A},\mathbf{p},\mu) &= n_\mathrm{R}\log\left(\frac{\sqrt{2\pi e}\sigma_{\max}}{\mathsf{A}} + \frac{1-e^{-\mu^*(\mathbf{p})}}{\mu^*(\mathbf{p})}\right) + \mu^*(\mathbf{p})\lambda(\mathbf{p}) - \mathsf{D}(\mathbf{p}\|\mathbf{q}) && (244)\\ &= n_\mathrm{R}\log\left(1+\frac{\mu^*(\mathbf{p})}{1-e^{-\mu^*(\mathbf{p})}}\cdot\frac{\sqrt{2\pi e}\sigma_{\max}}{\mathsf{A}}\right)\\ &\quad + n_\mathrm{R}\left(1-\log\left(\frac{\mu^*(\mathbf{p})}{1-e^{-\mu^*(\mathbf{p})}}\right) - \frac{\mu^*(\mathbf{p})\,e^{-\mu^*(\mathbf{p})}}{1-e^{-\mu^*(\mathbf{p})}}\right) - \mathsf{D}(\mathbf{p}\|\mathbf{q}) && (245)\\ &\le \sup_{\mathbf{p}\colon \frac{\lambda(\mathbf{p})}{n_\mathrm{R}}\in\left(\mathsf{A}^{\zeta-1},\frac{1}{2}\right)} \Biggl\{-\mathsf{D}(\mathbf{p}\|\mathbf{q}) + n_\mathrm{R}\log\left(1+\frac{\mu^*(\mathbf{p})}{1-e^{-\mu^*(\mathbf{p})}}\cdot\frac{\sqrt{2\pi e}\sigma_{\max}}{\mathsf{A}}\right)\\ &\qquad + n_\mathrm{R}\left(1-\log\left(\frac{\mu^*(\mathbf{p})}{1-e^{-\mu^*(\mathbf{p})}}\right) - \frac{\mu^*(\mathbf{p})\,e^{-\mu^*(\mathbf{p})}}{1-e^{-\mu^*(\mathbf{p})}}\right)\Biggr\} && (246)\\ &\triangleq g_1(\mathsf{A}). && (247) \end{aligned}$$

Here, in (245) we have used (233).

For the second case where $\frac{\lambda(\mathbf{p})}{n_\mathrm{R}} \le \mathsf{A}^{-(1-\zeta)}$, we use this inequality in combination with (232) to bound

$$\mu\lambda(\mathbf{p}) \le \mathsf{A}^{1-\zeta}\cdot n_\mathrm{R}\mathsf{A}^{-(1-\zeta)} = n_\mathrm{R}. \tag{248}$$

Because $\mathsf{D}(\mathbf{p}\|\mathbf{q}) \ge 0$, we thus obtain

$$\begin{aligned} g(\mathsf{A},\mathbf{p},\mu) &\le n_\mathrm{R}\log\left(\frac{\sqrt{2\pi e}\sigma_{\max}}{\mathsf{A}} + \frac{1-e^{-\mu}}{\mu}\right) + n_\mathrm{R} && (249)\\ &= n_\mathrm{R}\log\left(\frac{\sqrt{2\pi e}\sigma_{\max}}{\mathsf{A}} + \frac{1-e^{-\mathsf{A}^{1-\zeta}}}{\mathsf{A}^{1-\zeta}}\right) + n_\mathrm{R} && (250)\\ &\triangleq g_2(\mathsf{A}). && (251) \end{aligned}$$

For the third case where $\frac{\lambda(\mathbf{p})}{n_\mathrm{R}} \ge \frac{1}{2}$, we have

$$\begin{aligned} g(\mathsf{A},\mathbf{p},\mu) &= n_\mathrm{R}\log\left(\frac{\sqrt{2\pi e}\sigma_{\max}}{\mathsf{A}} + \frac{1-e^{-\frac{1}{\mathsf{A}}}}{\frac{1}{\mathsf{A}}}\right) + \frac{\lambda(\mathbf{p})}{\mathsf{A}} - \mathsf{D}(\mathbf{p}\|\mathbf{q}) && (252)\\ &\le n_\mathrm{R}\log\left(\frac{\sqrt{2\pi e}\sigma_{\max}}{\mathsf{A}} + \frac{1-e^{-\frac{1}{\mathsf{A}}}}{\frac{1}{\mathsf{A}}}\right) + \frac{\alpha}{\mathsf{A}} - \inf_{\mathbf{p}\colon \frac{\lambda(\mathbf{p})}{n_\mathrm{R}} > \frac{1}{2}} \mathsf{D}(\mathbf{p}\|\mathbf{q}) && (253)\\ &\triangleq g_3(\mathsf{A}). && (254) \end{aligned}$$

Here, we used (231) to bound $\lambda(\mathbf{p}) \le \alpha$.

We have now established (243) for the three functions defined in (247), (251), and (254), respectively. We now analyze the maximum in (243) when $\mathsf{A} \to \infty$. Since $g_2(\mathsf{A})$ tends to $-\infty$ as $\mathsf{A} \to \infty$, and since $g_1(\mathsf{A})$ and $g_3(\mathsf{A})$ are both bounded from below for $\mathsf{A} \ge 1$, we know that, for large enough A, $g_2(\mathsf{A})$ is strictly smaller than $\max\{g_1(\mathsf{A}), g_3(\mathsf{A})\}$.

We next look at $g_3(\mathsf{A})$ when $\mathsf{A} \to \infty$. Note that

$$\lim_{\mathsf{A}\to\infty} \frac{1-e^{-\frac{1}{\mathsf{A}}}}{\frac{1}{\mathsf{A}}} = 1, \tag{255}$$

therefore

$$\lim_{\mathsf{A}\to\infty} g_3(\mathsf{A}) = -\inf_{\mathbf{p}\colon \frac{\lambda(\mathbf{p})}{n_\mathrm{R}} > \frac{1}{2}} \mathsf{D}(\mathbf{p}\|\mathbf{q}) \tag{256}$$

$$= - \inf_{\mathbf{p}\colon \alpha - \sum_{\mathcal{I}\in\mathcal{U}} p_{\mathcal{I}} s_{\mathcal{I}} \geq \frac{n_{\mathrm{R}}}{2}} \mathsf{D}(\mathbf{p}\|\mathbf{q}) \tag{257}$$

$$= - \inf_{\mathbf{p}\colon \alpha - \sum_{\mathcal{I}\in\mathcal{U}} p_{\mathcal{I}} s_{\mathcal{I}} = \frac{n_{\mathrm{R}}}{2}} \mathsf{D}(\mathbf{p}\|\mathbf{q}), \tag{258}$$

where the last equality holds because given $\alpha < \alpha_{\mathrm{th}}$, an optimal $\mathbf{p}$ will meet the constraint with equality.

It remains to investigate the behavior of $g_1(\mathsf{A})$ when $\mathsf{A} \to \infty$. To this end, we define

$$\begin{aligned} \tilde{g}_1(\mathsf{A}, \mathbf{p}) \triangleq{} & -\mathsf{D}(\mathbf{p}\|\mathbf{q}) + n_{\mathrm{R}} \log\left(1 + \frac{\mu^*(\mathbf{p})}{1 - e^{-\mu^*(\mathbf{p})}} \cdot \frac{\sqrt{2\pi e}\sigma_{\max}}{\mathsf{A}}\right) \\ & + n_{\mathrm{R}} \left(1 - \log\left(\frac{\mu^*(\mathbf{p})}{1 - e^{-\mu^*(\mathbf{p})}}\right) - \frac{\mu^*(\mathbf{p})\, e^{-\mu^*(\mathbf{p})}}{1 - e^{-\mu^*(\mathbf{p})}}\right), \end{aligned} \tag{259}$$

and note that, for any fixed $\mathbf{p}$,

$$\Delta(\mathsf{A}, \mathbf{p}) \triangleq \tilde{g}_1(\mathsf{A}, \mathbf{p}) - \lim_{\mathsf{A}\to\infty} \tilde{g}_1(\mathsf{A}, \mathbf{p}) = \log\left(1 + \frac{\mu^*(\mathbf{p})}{1 - e^{-\mu^*(\mathbf{p})}} \cdot \frac{\sqrt{2\pi e}\sigma_{\max}}{\mathsf{A}}\right). \tag{260}$$

Since, when $\mathsf{A} \to \infty$,

$$|\Delta(\mathsf{A}, \mathbf{p})| \leq \log\left(1 + \left|\frac{1}{1 - e^{-\mathsf{A}^{1-\zeta}}} \cdot \frac{\sqrt{2\pi e}\sigma_{\max}}{\mathsf{A}^{\zeta}}\right|\right) \to \log(1) = 0, \tag{261}$$

we see that $\tilde{g}_1(\mathsf{A}, \mathbf{p})$ converges uniformly over $\mathbf{p}$ as $\mathsf{A} \to \infty$, and therefore we are allowed to interchange limit and supremum:

$$\begin{aligned} & \lim_{\mathsf{A}\to\infty} g_1(\mathsf{A}) \\ & = \lim_{\mathsf{A}\to\infty} \sup_{\mathbf{p}\colon \frac{\lambda(\mathbf{p})}{n_{\mathrm{R}}} \in \left(\mathsf{A}^{\zeta-1}, \frac{1}{2}\right)} \tilde{g}_1(\mathsf{A}, \mathbf{p}) && (262) \\ & = \sup_{\mathbf{p}\colon \frac{\lambda(\mathbf{p})}{n_{\mathrm{R}}} \in \left(0, \frac{1}{2}\right)} \lim_{\mathsf{A}\to\infty} \tilde{g}_1(\mathsf{A}, \mathbf{p}) && (263) \\ & = \sup_{\mathbf{p}\colon \frac{\lambda(\mathbf{p})}{n_{\mathrm{R}}} \in \left(0, \frac{1}{2}\right)} \left\{ n_{\mathrm{R}} \left(1 - \log \frac{\mu^*(\mathbf{p})}{1 - e^{-\mu^*(\mathbf{p})}} - \frac{\mu^*(\mathbf{p})\, e^{-\mu^*(\mathbf{p})}}{1 - e^{-\mu^*(\mathbf{p})}}\right) - \mathsf{D}(\mathbf{p}\|\mathbf{q}) \right\} && (264) \\ & = \sup_{\mathbf{p}\colon \lambda(\mathbf{p}) \in \left(\max\{0, \frac{n_{\mathrm{R}}}{2} + \alpha - \alpha_{\mathrm{th}}\}, \min\{\frac{n_{\mathrm{R}}}{2}, \alpha\}\right)} \left\{ n_{\mathrm{R}} \left(1 - \log \frac{\mu^*(\mathbf{p})}{1 - e^{-\mu^*(\mathbf{p})}} - \frac{\mu^*(\mathbf{p})\, e^{-\mu^*(\mathbf{p})}}{1 - e^{-\mu^*(\mathbf{p})}}\right) \right. \\ & \qquad \left. - \mathsf{D}(\mathbf{p}\|\mathbf{q}) \right\} && (265) \\ & = \nu. && (266) \end{aligned}$$

Here, in (265) we are allowed to restrict the supremum[3] to $\lambda(\mathbf{p}) \in (\frac{n_{\mathrm{R}}}{2} + \alpha - \alpha_{\mathrm{th}}, \alpha)$ because of (231) and because

$$\lambda(\mathbf{q}) \triangleq \alpha - \sum_{\mathcal{I}\in\mathcal{U}} s_{\mathcal{I}} q_{\mathcal{I}} = \alpha - \alpha_{\mathrm{th}} + \frac{n_{\mathrm{R}}}{2} \tag{267}$$

and for any $\mathbf{p}$ such that $\lambda(\mathbf{p}) \leq \lambda(\mathbf{q})$ the objective function in (264) is smaller than for $\mathbf{p} = \mathbf{q}$. In fact, $-\mathsf{D}(\mathbf{p}\|\mathbf{q})$ is clearly maximized for $\mathbf{p} = \mathbf{q}$ and

$$\mu^*(\mathbf{p}) \mapsto n_{\mathrm{R}} \left(1 - \log \frac{\mu^*(\mathbf{p})}{1 - e^{-\mu^*(\mathbf{p})}} - \frac{\mu^*(\mathbf{p})\, e^{-\mu^*(\mathbf{p})}}{1 - e^{-\mu^*(\mathbf{p})}}\right) \tag{268}$$

[3]Notice that because of the supremum and continuity, we can restrict to the open interval instead of the closed interval.

is decreasing in $\mu^*(\mathbf{p})$, which is a decreasing function of $\lambda(\mathbf{p})$; see (233). Finally, (266) follows from the definition of ν in (68).

It is straightforward to see that ν is larger than the RHS of (258). Therefore,

$$\lim_{\mathsf{A}\to\infty} \max\{g_1(\mathsf{A}), g_2(\mathsf{A}), g_3(\mathsf{A})\} = \nu. \tag{269}$$

Combining (237) with (241), (243), and (269) proves the theorem.

F.2 Proof of Theorem 21

From [23, Corollary 2], it is known that the capacity is lower-bounded as

$$\mathsf{C_H}(\mathsf{A}, \alpha\mathsf{A}) \geq \frac{1}{2} \max_{P_{\bar{\mathbf{X}}}} \operatorname{tr}\bigl(\mathsf{K}_{\bar{\mathbf{X}}\bar{\mathbf{X}}}\bigr) + o\biggl(\max_{P_{\bar{\mathbf{X}}}} \operatorname{tr}\bigl(\mathsf{K}_{\bar{\mathbf{X}}\bar{\mathbf{X}}}\bigr)\biggr). \tag{270}$$

For an upper bound, we use that

$$\log(1+\xi) \leq \xi, \quad \xi > 0, \tag{271}$$

and obtain from Theorem 19 that

$$\mathsf{C_H}(\mathsf{A}, \alpha\mathsf{A}) \leq \frac{1}{2} \max_{P_{\bar{\mathbf{X}}}} \operatorname{tr}\bigl(\mathsf{K}_{\bar{\mathbf{X}}\bar{\mathbf{X}}}\bigr). \tag{272}$$

The theorem is proven by normalizing $\bar{\mathbf{X}}$ by A, which results in a factor A^2, and by then letting A go to zero.

References

[1] Mohammad Ali Khalighi and Murat Uysal, "Survey on free space optical communication: A communication theory perspective," *IEEE Comm. Surveys & Tutorials*, vol. 16, no. 4, pp. 2231–2258, fourth quarter 2014.

[2] Dilukshan Karunatilaka, Fahad Zafar, Vineetha Kalavally, and Rajendran Parthiban, "LED based indoor visible light communications: State of the art," *IEEE Comm. Surveys & Tutorials*, vol. 17, no. 3, pp. 1649–1678, third quarter 2015.

[3] Murat Uysal and Hatef Nouri, "Optical wireless communications – an emerging technology," in *Proc. IEEE Int. Conf. Transp. Optical Netw.*, Graz, Austria, Jul. 6–10, 2014, pp. 1–7.

[4] Michèle A. Wigger, "Bounds on the capacity of free-space optical intensity channels," Master's thesis, Signal and Inf. Proc. Lab., ETH Zürich, Switzerland, Mar. 2003.

[5] Amos Lapidoth, Stefan M. Moser, and Michèle A. Wigger, "On the capacity of free-space optical intensity channels," *IEEE Trans. Inf. Theory*, vol. 55, no. 10, pp. 4449–4461, Oct. 2009.

[6] Andrew L. McKellips, "Simple tight bounds on capacity for the peak-limited discrete-time channel," in *Proc. IEEE Int. Symp. Inf. Theory*, Chicago, IL, USA, Jun. 27 – Jul. 2, 2004, p. 348.

[7] Andrew Thangaraj, Gerhard Kramer, and Georg Böcherer, "Capacity bounds for discrete-time, amplitude-constrained, additive white Gaussian noise channels," *IEEE Trans. Inf. Theory*, vol. 63, no. 7, pp. 4172–4182, Jul. 2017.

[8] Borzoo Rassouli and Bruno Clerckx, "An upper bound for the capacity of amplitude-constrained scalar AWGN channel," *IEEE Commun. Lett.*, vol. 20, no. 10, pp. 1924–1926, Oct. 2016.

[9] Stefan M. Moser, Ligong Wang, and Michèle Wigger, "Asymptotic high-SNR capacity of MISO optical intensity channels," in *Proc. IEEE Inf. Theory Workshop*, Kaohsiung, Taiwan, Nov. 6–10, 2017, pp. 86–90.

[10] Stefan M. Moser, Ligong Wang, and Michèle Wigger, "Capacity results on multiple-input single-output wireless optical channels," *IEEE Trans. Inf. Theory*, vol. 64, no. 11, pp. 6954–6966, Nov. 2018.

[11] Stefan M. Moser, Michail Mylonakis, Ligong Wang, and Michèle Wigger, "Asymptotic capacity results for MIMO wireless optical communication," in *Proc. IEEE Int. Symp. Inf. Theory*, Aachen, Germany, Jun. 25–30, 2017, pp. 536–540.

[12] Anas Chaaban, Zouheir Rezki, and Mohamed-Slim Alouini, "MIMO intensity-modulation channels: Capacity bounds and high SNR characterization," in *Proc. IEEE Int. Conf. Commun.*, Paris, France, May 21–25, 2017, pp. 1–6.

[13] Anas Chaaban, Zouheir Rezki, and Mohamed-Slim Alouini, "Capacity bounds and high-SNR capacity of MIMO intensity-modulation optical channels," *IEEE Trans. Wireless Commun.*, vol. 17, no. 5, pp. 3003–3017, May 2018.

[14] Alex Dytso, Mario Goldenbaum, Shlomo Shamai, and H. Vincent Poor, "Upper and lower bounds on the capacity of amplitude-constrained MIMO channels," in *Proc. IEEE Global Commun. Conf.*, Singapore, Dec. 4–8, 2017, pp. 1–6.

[15] Anas Chaaban, Zouheir Rezki, and Mohamed-Slim Alouini, "Low-SNR asymptotic capacity of MIMO optical intensity channels with peak and average constraints," *IEEE Trans. Commun.*, vol. 66, no. 10, pp. 4694–4705, Oct. 2018.

[16] Zixiong Wang, Wen-De Zhong, Songnian Fu, and Chinlon Lin, "Performance comparison of different modulation formats over free-space optical (FSO) turbulence links with space diversity reception technique," *IEEE Photonics J.*, vol. 1, no. 6, pp. 277–285, Dec. 2009.

[17] Ertugrul Başar, Erdal Panayirci, Murat Uysal, and Harald Haas, "Generalized LED index modulation optical OFDM for MIMO visible light communications systems," in *Proc. IEEE Int. Conf. Commun.*, Kuala Lumpur, Malaysia, May 23–27, 2016, pp. 1–5.

[18] Anil Yesilkaya, Ertugrul Basar, Farshad Miramirkhani, Erdal Panayirci, Murat Uysal, and Harald Haas, "Optical MIMO-OFDM with generalized LED index modulation," *IEEE Trans. Commun.*, vol. 65, no. 8, pp. 3429–3441, Aug. 2017.

[19] Shane M. Haas, Jeffrey H. Shapiro, and Vahid Tarokh, "Space-time codes for wireless optical communications," *EURASIP J. App. Sig. Proc.*, no. 3, pp. 211–220, 2002.

[20] Ehsan Bayaki and Robert Schober, "On space–time coding for free–space optical systems," *IEEE Trans. Commun.*, vol. 58, no. 1, pp. 58–62, Jan. 2010.

[21] Xuegui Song and Julian Cheng, "Subcarrier intensity modulated MIMO optical communications in atmospheric turbulence," *IEEE/OSA J. of Optical Comm. & Networking*, vol. 5, no. 9, pp. 1001–1009, Sept. 2013.

[22] Thomas M. Cover and Joy A. Thomas, *Elements of Information Theory*, 2nd ed. New York, NY, USA: Wiley, 2006.

[23] Vyacheslav V. Prelov and Sergio Verdú, "Second-order asymptotics of mutual information," *IEEE Trans. Inf. Theory*, vol. 50, no. 8, pp. 1567–1580, Aug. 2004.

[24] Ram Zamir and Meir Feder, "On the volume of the Minkowski sum of line sets and the Entropy-Power Inequality," *IEEE Trans. Inf. Theory*, vol. 44, no. 7, pp. 3039–3043, Nov. 1998.

[25] Geoffrey C. Shephard, "Combinatorial properties of associated zonotopes," *Canad. J. Math.*, vol. 26, no. 2, pp. 302–321, Feb. 1974.

[26] Stefan M. Moser, *Information Theory (Lecture Notes)*, 6th ed. Signal and Inf. Proc. Lab., ETH Zürich, Switzerland, and Inst. Commun. Eng., Nat. Chiao Tung Univ., Hsinchu, Taiwan, 2018. Available: http://moser-isi.ethz.ch/scripts.html